Computers and Concrete, *Vol. 26, No. 1* (*2020*) *31-52*
DOI: https://doi.org/10.12989/cac.2020.26.1.031

Vibration analysis of porous nanocomposite viscoelastic plate reinforced by FG-SWCNTs based on a nonlocal strain gradient theory

Pegah Khazaei and Mehdi Mohammadimehr*

Department of Solid Mechanics, Faculty of Mechanical Engineering, University of Kashan, Kashan, Iran

(*Received March 4, 2020, Revised May 26, 2020, Accepted June 1, 2020*)

Abstract. This paper investigates the size dependent effect on the vibration analysis of a porous nanocomposite viscoelastic plate reinforced by functionally graded-single walled carbon nanotubes (FG-SWCNTs) by considering nonlocal strain gradient theory. Therefore, using energy method and Hamilton's principle, the equations of motion are derived. In this article, the effects of nonlocal parameter, aspect ratio, strain gradient parameter, volume fraction of carbon nanotubes (CNTs), damping coefficient, porosity coefficient, and temperature change on the natural frequency are perused. The innovation of this paper is to compare the effectiveness of each mentioned parameters individually on the free vibrations of this plate and to represent the appropriate value for each parameter to achieve an ideal nanocomposite plate that minimizes vibration. The results are verified with those referenced in the paper. The results illustrate that the effect of damping coefficient on the increase of natural frequency is significantly higher than the other parameters effect, and the effects of the strain gradient parameter and nonlocal parameter on the natural frequency increase are less than damping coefficient effect, respectively. Furthermore, the results indicate that the natural frequency decreases with a rise in the nonlocal parameter, aspect ratio and temperature change. Also, the natural frequency increases with a rise in the strain gradient parameter and CNTs volume fraction. This study can be used for optimizing the industrial and medical designs, such as automotive industry, aerospace engineering and water purification system, by considering ideal properties for the nanocomposite plate.

Keywords: vibration analysis; porous materials; nanocomposite; carbon nanotube; nonlocal strain gradient theory; Hamilton's principle; viscoelasticity

1. Introduction

Nanoscience has extensive applications in different fields of nanotechnology. For instance, it can be used in these branches: cements in buildings, water purification, new fuels for energy production, materials with new properties for aeronautics and etcetera. Carbon nanotubes (CNTs) are recognized as one of the most important constituents of composite structures in nanotechnology. For further investigation, CNTs are assumed as very strong and stiff from the point of view of tensile strength and elastic modulus. Due to these special properties, CNTs were used widely in order to strengthen the composites. In addition to CNTs, porous materials also improve the properties of composites. Nowadays, the use of lightweight materials especially porous materials is taken into consideration owing to be cost-effectively, structure weight reduction, recycling potential and special heat transfer potential.

Various theories can be used to study the properties and behavior of porous and CNTs-reinforced composites, including nonlocal strain gradient theory. Among the researches using nonlocal strain gradient theory, these studies can be noted: Malikan *et al.* (2018a) investigated the damped forced vibration analysis of single-walled carbon nanotubes (SWCNTs) resting on viscoelastic foundation in thermal environment using nonlocal strain gradient theory. The equilibrium equations are formulated by the new shear deformation beam theory which is accompanied with higher-order nonlocal strain gradient theory. Arefi *et al.* (2019) discussed bending analysis of a sandwich porous nanoplate in order to study the size dependent effect via nonlocal strain gradient theory. The results represented that non-dimensional displacement of nanoplate increases with the increase of nonlocal parameter. She *et al.* (2018b) through nonlocal strain gradient theory, proposed nonlinear bending and vibration analysis of functionally graded (FG) porous tubes. Malikan (2020) using strain gradient elasticity theory, predicted theoretically static stability response of a curved carbon nanotube under an elastoplastic behavior. He illustrated that the variation of nonlocal and strain gradient parameters lead to softening and hardening into both elasticity and plasticity regions. Rajabi and Mohammadimehr (2019) considered bending analysis of a micro sandwich skew plate using extended Kantorovich method based on Eshelby-Mori-Tanaka approach. Gao *et al.* (2019) studied the nonlinear vibration of beams subjected to different types of functionally graded (FG) distribution using nonlocal strain gradient theory. Ebrahimi *et al.* (2019b) investigated wave propagation-thermal characteristics of a size-dependent graphene nanoplatelet-reinforced composite (GNPRC) porous cylindrical nanoshell using nonlocal strain gradient theory. They analyzed the effects of small scale. Moreover, in their

*Corresponding author, Associate Professor
E-mail: mmohammadimehr@kashanu.ac.ir

ISSN: 1598-8198 (Print), 1598-818X (Online)

research, Hamilton's principle is used to evolve the governing equations. Also (Lu *et al.* 2019, Ebrahimi and Barati 2018, Ebrahimi and Dabbagh 2017) have done research based on nonlocal strain gradient theory.

Many studies as the present article through Hamilton's principle and energy method have obtained equations of motion in order to peruse vibration, bending and buckling analysis of nanocomposites with various properties. Thai and Choi (2013) inquired the effect of the strain gradient parameter on the bending, buckling, and vibration responses of FG Kirchhoff and Mindlin plates using Hamilton's principle based on a modified couple stress theory. Also Mohammadimehr *et al.* (2018a) investigated the free vibration and buckling analyses of double-bonded micro composite sandwich reinforced by CNTs and boron nitride nanotubes (BNNTs) using most general strain gradient theory (MGSGT), sinusoidal shear deformation theory (SSDT) and also by employing Hamilton's principle and energy method in order to obtain the equations of motion,. Moreover, (Jafarian Arani and Kolahchi 2016, Mohammadimehr *et al.* 2016c, Ebrahimi and Dabbagh 2019, Bousahla *et al.* 2020, Moradi Dastjerdi *et al.* 2017) have gained equations of motion via Hamilton's principle and energy method. AkhavanAlavi *et al*. (2019) presented active control of micro Reddy beam integrated with functionally graded nanocomposite sensor and actuator based on linear quadratic regulator (LQR) method.

Among vibration analysis in view of various types of plate theories, these articles are noteworthy: Mohammadimehr *et al.* (2016b) inquired bending, buckling and vibration analysis of a microcomposite plate reinforced by FG-SWCNT via modified strain gradient theory (MSGT), third-order shear deformation theory (TSDT). Furthermore, Ebrahimi and Shafiei (2017) using Reddy's higher-order shear deformation plate theory, studied the small scale effect on the vibration behavior of orthotropic single layered graphene sheets. The results revealed that the nonlocal effect increases as the size of the graphene sheet is decreased. It is also found that the frequency ratios decrease with an increase in vibration modes. Also, Zenkour and Alghanmi (2019) via four-unknown shear deformation theory, brought up the stress analysis of a FG plate integrated with piezoelectric faces. Furthermore, Mohammadimehr *et al.* (2015) proposed free vibration of viscoelastic double-bonded polymeric nanocomposite plates reinforced by FG-SWCNTs using MSGT, sinusoidal shear deformation theory and meshless method. Also Ebrahimi and Farazmandnia (2017) for free vibration analysis of functionally graded carbon nanotube-reinforced composite (FG-CNTRC) sandwich, proposed a higher-order shear deformation beam theory (HSBT). They derived the governing equations and boundary conditions by using Hamilton's principle and the Navier solution procedure is used to achieve the natural frequencies of the sandwich beam. Numerical results indicated that volume fraction of CNT, has considerable effects on the natural frequencies. It is found that the natural frequencies of the sandwich beam decrease with an increase in temperature change and vice versa for the volume fraction of CNT. In addition, (Mousavi *et al*. 2019, Ghorbanpour-Arani and Jalaei 2017, Rezaei *et al.* 2017, Van Do *et al.* 2017, Mohammadimehr and Alimirzaei 2016) can be pointed out as investigations which have used different theories for vibration, bending and buckling analysis.

To illustrate the effects of nonlocal and strain gradient parameters and size effects. Ebrahimi *et al.* (2019a) using nonlocal elasticity theory and modified couple stress theory, captured the size effects for analyzing the static stability and natural frequencies of FG nanobeams. Their results demonstrated that effect of nonlocal parameter on frequencies of nonlocal couple stress FG nanobeams depends on the value of slenderness ratio. Malikan and Eremeyev (2020b) by considering the surface, nonlocal and small size influences, perused the post-critical stability response of a truncated conical carbon nanotube by taking the nonlinear Winkler elastic substrate. Their results demonstrated that clamped-simply-supported (CS) and simply supported (SS) boundary conditions are influenced by the surface effect more than other ones. Thai and Kim (2013) perused the effects of small scale on the responses of microplates. Their results demonstrated that the inclusion of small scale effects results in an increase in plate stiffness and it causes a reduction in deflection and an increase in frequency. Ghorbanpour Arani *et al*. (2016) illustrated surface stress and agglomeration effects on nonlocal biaxial buckling polymeric nanocomposite plate reinforced by CNT using various approaches. Further, the effects of boundary conditions, small scale and aspect ratio on the critical buckling load of SWCNTs were analyzed by Ansari *et al.* (2015). Mohammadimehr *et al*. (2017a, b) considered nonlinear vibration analysis of FG-CNTRC sandwich Timoshenko beam based on modified couple stress theory and dynamic stability of modified strain gradient theory sinusoidal viscoelastic piezoelectric polymeric functionally graded single-walled carbon nanotubes reinforced nanocomposite plate, respectively. Akbarzadeh Khorshidi (2018) presented the material length scale parameter used in couple stress theory and proved that this parameter cannot be a material constant and its value depends on the different physical and natural conditions. Kim *et al.* (2019) have also done research in this case. They presented numerical results of bending, free vibration, and buckling of a FG porous microplates to determine the effects of microstructure-dependent size effects using the modified couple stress theory. They illustrated that the strain gradient parameter can capture microstructure size effects (stiffening effects).

In case of viscoelasticity, Li *et al.* (2016) using nonlocal strain gradient theory, perused the wave propagation in viscoelastic SWCNTs under magnetic field. It can be comprehended from results that the size-dependent effects on the phase velocity is significant at high wave numbers however, it can be ignored at low wave numbers. Also the damping ratio considering surface effect is larger than that without considering surface effect. Furthermore, Malikan and Eremeyev (2020a) incorporated viscoelasticity into a piezoelectric–flexoelectric Euler–Bernoulli nanobeam, while Kelvin–Voigt linear viscoelastic coupling was applied to the dynamic analysis. They measured the natural frequencies in nanoscale by using the nonlocal strain gradient elasticity model. The results reveal that by

increasing the inner viscoelastic values, the role of flexoelectricity becomes greater and also by increasing the values of strain gradient parameter, the inner viscoelastic impact becomes greater. Mohammadimehr *et al*. (2016d) depicted size-dependent effect on biaxial and shear nonlinear buckling analysis of nonlocal isotropic and orthotropic micro-plate based on surface stress and modified couple stress theories using differential quadrature method. Also Malikan *et al.* (2019) using modified Timoshenko's beam theory and a nonlocal strain gradient model, investigated vibrational behavior of a carbon nanotube in the presence of internal and external viscoelasticity. They demonstrated that the external damping increases the damping rate of the system, while the internal damping reduces the amplitudes of the motion.

Many scholars have done research on porous materials as Rezaei and Saidi (2015). They inquired the free vibration analysis for thick rectangular porous plate. The results revealed that the natural frequency of fluid free plates decreases as the plate's porosity increases. Malikan *et al.* (2018c) investigated the buckling of rectangular functionally graded porous nanoplates based on three-dimensional elasticity. Their results illustrated that even porosity makes the plate softer and results of uneven porosity are so close to the prefect material which leads to this considerable conclusion that porosity as an uneven distribution cannot be an important factor in static stability analyses. Also Yang *et al.* (2018) perused the buckling and free vibration behaviors of FG porous nanocomposite plates reinforced with graphene platelets (GPLs). They indicated that by increasing the porosity coefficient, the uniaxial, biaxial and shear buckling loads and also the fundamental natural frequencies of the proposed plates, decrease. Dinh Duc *et al.* (2018) by considering two types of porosity including evenly distributed porosities (Porosity-I) and unevenly distributed porosities (Porosity-II) to study the nonlinear dynamic response of porous functionally graded material (FGM) plates on the elastic foundation based on the first order shear deformation theory. Their results indicated that the value of the natural frequency of FGM plates in the case Porosity-I is lower than that in Porosity-II phase. Moreover, Ebrahimi and Barati (2017) presented the size-dependent and porosity-dependent vibrational behavior of magneto-electro-elastic functionally graded (MEE-FG) nanoscale beams. They considered Eringen's nonlocal elasticity theory to capture the small size effects. Their results illustrated that the nonlocal parameter yields in reduction in both rigidity of the beam and natural frequencies. Besides, (Amir *et al.* 2019, She *et al.* 2018a, Addou *et al.* 2019, Kaddari *et al.* 2020) have carried out some investigations into porous materials.

Among the studies in the field of various FG distributions, Mohammadimehr *et al.* (2016c) revealed that the FG-X and FG-O patterns of SWCNTs cause the highest and lowest dimensionless buckling loads and vice versa for deflection. In addition, Ebrahimi *et al.* (2019c) inferred that reinforcing the plate with X-type distribution leads to a higher range of the dimensionless natural frequencies followed by *U*, *V* and *O* types in thermal vibration analysis of embedded graphene oxide powder reinforced nanocomposite plates.

Furthermore, to study the piezoelectric properties of composites, these probes can be taken into account: Ghorbanpour Arani *et al.* (2016) by assuming four different types of FG distribution patterns of SWCNTs reinforcements, investigated the nonlocal wave propagation analysis of embedded nanocomposite polymeric piezoelectric micro plates reinforced by SWCNTs. Their investigation can be used for optimum design of smart composite plates as micro-electro-magneto-mechanical sensors. Also Arefi *et al.* (2018) proposed the free vibration analysis of a piezoelectric curved sandwich nanobeam with FG carbon nanotube reinforcement composites face-sheets. Moreover, Zhang *et al.* (2018) proposed semi-analytical solutions for vibration analysis of nonlocal piezoelectric Kirchhoff plates resting on viscoelastic foundation. Their results indicated that by raising the external electric voltage, the natural frequencies of plates with various boundary conditions decrease and the effect of external electric voltage becomes significant as the nonlocal parameter is applied. Further, (Gholami and Ansari 2017, Tanzadeh and Amoushahi 2019) have done researches in case of piezoelectric nanocomposites.

According to the aforesaid researches, vibration analysis of the nanocomposite plate have been developed and investigated by some researchers, but no literature has been reported for vibration analysis of porous nanocomposite viscoelastic plate reinforced by FG-SWCNTs based on a nonlocal strain gradient theory. On the other hands, despite the fact that many researchers have been done in case of nonlocal strain gradient theory and vibration analysis of the nanocomposite plate which composed by CNTs as above-mentioned studies, what distinguishes this paper from other articles is that by studying the effect of different properties on the vibrations of this system, one can achieve a set of ideal properties that dramatically reduce the vibrations of the system which is very significant in optimizing the design. This paper considers simultaneously diverse properties for FG-SWCNTs-reinforced nanocomposite plate such as: porosity, piezoelectric and viscoelastic features and with the help of nonlocal strain gradient theory and energy method that is novelty of this research. Also, vibration analysis is performed on a nanocomposite plate with the specified properties. For this purpose, the effects of nonlocal parameter, aspect ratio, strain gradient parameter, volume fraction of CNTs, damping coefficient, porosity coefficient, temperature change and various FG-SWCNTs distribution patterns on the natural frequency have been investigated.

2. Geometry of porous nanocomposite viscoelastic plate reinforced by FG-SWCNTs

Consider a porous nanocomposite viscoelastic and piezoelectric rectangular plate of length *a*, width *b* and total thickness *h* and composed of FG-SWCNTs as shown in Fig. 1.

Fig. 2 shows the various distribution patterns (uniform distribution (UD), FG-X, FG-O and FG-V) of the FG-SWCNTs along the thickness direction. Eq. (1) illustrates the volume fraction $V_{CNT}$of various SWCNTs distributions

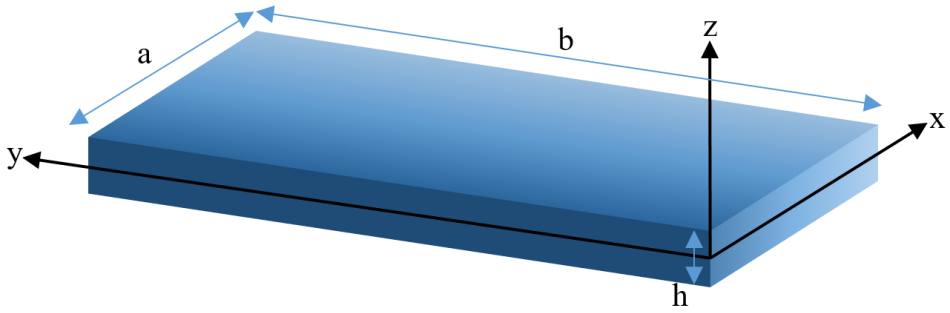

Fig. 1 A schematic view of porous nanocomposite viscoelastic and piezoelectric plate reinforced by carbon nanotubes

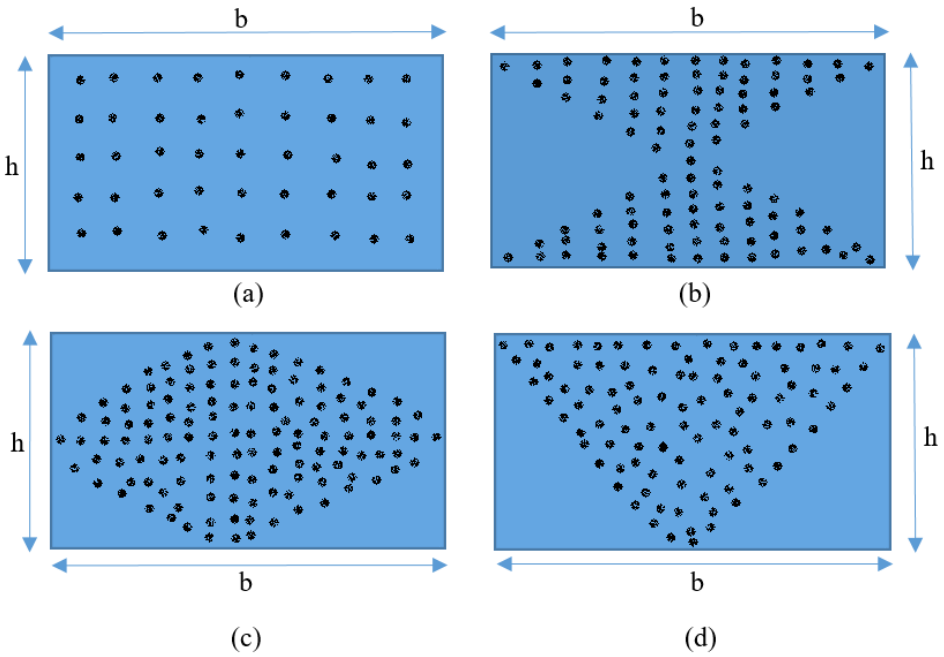

Fig. 2 (a) A schematic view of UD CNTs distribution. (b) A schematic view of FG-X CNTs distribution. (c) A schematic view of FG-O CNTs distribution. (c) A schematic view of FG-V CNTs distribution

as follows (Mohammadimehr *et al.* 2016b):

$$V_{CNT}(z)=\begin{cases} V_{CNT}^{*} & (UD \quad CNTRC), \\ \left(1+\dfrac{2z}{h}\right)V_{CNT}^{*} & (FG-V \quad CNTRC), \\ 2\left(1-\dfrac{|2z|}{h}\right)V_{CNT}^{*} & (FG-O \quad CNTRC), \\ V_{r}=2\dfrac{|2z|}{h}V_{CNT}^{*} & (FG-X \quad CNTRC), \end{cases} \tag{1}$$

where

$$V_{CNT}^{*}=\frac{w_{CNT}}{w_{CNT}+\left(\rho^{CNT}/\rho^{m}\right)-\left(\rho^{CNT}/\rho^{m}\right)w_{CNT}}, \tag{2}$$

in which ρ^{CNT} and ρ^{m} are the densities of SWCNTs and Polyvinylidene fluoride (PVDF) nanoplate matrix, respectively and W_{CNT} is the mass fraction of nanotube. $V_{CNT}(z)$ and V_{CNT}^{*} are the various distributions of CNT including UD, FG-V, FG-O, FG-X and volume fraction of CNT, respectively.

3. Material properties

3.1 The extended rule of mixture approach

In order to predict the mechanical-moisture-thermal properties of nanocomposite plate reinforced by SWCNTs, the extended rule of mixture (ERM) approach has been used. According to this approach, mentioned properties are acquired from the following equations (Mohammadimehr *et al.* 2016b)

$$\begin{aligned} E_{11}&=\eta_{1}V_{CNT}E_{11}^{CNT}+V_{m}E_{m}, \\ \frac{\eta_{2}}{E_{22}}&=\frac{V_{CNT}}{E_{22}^{CNT}}+\frac{V_{m}}{E_{m}}, \\ \frac{\eta_{3}}{G_{12}}&=\frac{V_{CNT}}{G_{12}^{CNT}}+\frac{V_{m}}{G_{m}}, \end{aligned} \tag{3}$$

where E_{11}^{CNT}, E_{22}^{CNT} and G_{12}^{CNT} present Young's modulus in various directions and shear modulus of SWCNTs, respectively and E_m and G_m are the Young's modulus and shear modulus related to PVDF matrix, respectively. η_i (i=1,2,3) is CNT efficiency parameter which specified by

Table 1 CNT efficiency parameters (Mohammadimehr *et al.* 2018)

V^*_{CNT}	0.11	0.14	0.17
η_1	0.149	0.150	0.149
η_2	0.934	0.941	1.381
η_3	0.934	0.941	1.381

Table 2 Mechanical properties of SWCNTs with υ_{CNT}=0.175 (Mohammadimehr *et al.* 2018)

Temperature (T_0)(κ)	300	400	500
E_{11}^{CNT} (TPa)	5.6466	5.5308	5.4744
E_{22}^{CNT} (TPa)	7.0800	6.9348	6.8641
G_{12}^{CNT} (TPa)	1.9445	1.9643	1.9644

Table 3 Properties of SWCNTs and PVDF nanoplate matrix (Mohammadimehr *et al.* 2018, (Mohammadimehr *et al.* 2016c, Ghorbanpour Arani *et al.* 2016)

PVDF nanoplate matrix	SWCNTs
$\upsilon_m = 0.18$	
$V_m = 0.89$	
$\rho_m = 1780\left(kg/m^3\right)$	$\upsilon_{CNT} = 0.175$
$\begin{cases} E_m = (3.51 - 0.0047T)\,(GPa) \\ T = T_0 + \Delta T\ (K) \end{cases}$	$V_{CNT} = 0.11$
$G_m = \dfrac{E_m}{2(1+\upsilon_m)}\,(GPa)$	$\rho_{CNT} = 1400\left(kg/m^3\right)$

molecular dynamic (MD) simulation. In fact, CNT efficiency parameters are the transformation forces between carbon nanotubes and matrix. V_m is volume fractions of PVDF nanoplate matrix. The relation between volume fractions of CNT and PVDF nanoplate matrix is defined by Alibeigloo (2013)

$$V_{CNT} + V_m = 1. \tag{4}$$

Also, the Poisson's ratio along the thickness direction and density of the composite plate are given by the following equations (Ghorbanpour Arani *et al.* 2016)

$$\upsilon_{12} = V^*_{CNT}\upsilon^{CNT} + V_m\upsilon^m, \tag{5}$$

$$\rho = V_{CNT}\rho^{CNT} + V_m\rho^m, \tag{6}$$

where υ^m and υ^{CNT} are Poisson's ratio of PVDF nanoplate matrix and SWCNTs, respectively.

The values of properties of SWCNTs and PVDF nanoplate matrix and CNT efficiency parameters are depicted in Tables 1-3.

3.2 Density and elasticity modulus of FG-SWCNTs-reinforced porous nanocomposite plate

The distribution of porosity along the thickness of plate in the porous nanocomposites is changeable therefore, density and elasticity modulus of FG-SWCNTs-reinforced porous nanocomposite plate are functions of the *Z* and they are obtained by following equations (Mohammadimehr *et al.* 2018, Mohammadimehr *et al.* 2016b, Rezaei and Saidi 2015)

$$\begin{cases} E_x(z) = E_{11}\left(1\text{-e}\cos\left(\dfrac{\pi}{2\text{h}}(\text{z}+\dfrac{h}{2})\right)\right), \\ E_y(z) = E_{22}\left(1\text{-e}\cos\left(\dfrac{\pi}{2\text{h}}(\text{z}+\dfrac{h}{2})\right)\right), \\ E_{xy}(z) = G_{12}\left(1\text{-e}\cos\left(\dfrac{\pi}{2\text{h}}(\text{z}+\dfrac{h}{2})\right)\right), \\ \rho(z) = \rho\left(1\text{-e}'\cos\left(\dfrac{\pi}{2\text{h}}(\text{z}+\dfrac{h}{2})\right)\right), \\ \text{e}' = 1-\sqrt{1-e}, \end{cases} \tag{7}$$

in which, e is porosity coefficient and the values of E_{11}, E_{22}, G_{12} and ρ are embedded using Eqs. (3), (6).

4. Problem formulation

For the sake of obtaining the governing motion equations from Hamilton's principle, energy method is used. For this purpose, displacement fields, strain-displacement equations of classical plate theory (CPT) and stress-strain equations of porous nanocomposite viscoelastic and piezoelectric plate composed of FG-SWCNTs are considered.

4.1 Nonlocal strain gradient theory for porous nanocomposite viscoelastic and piezoelectric plate reinforced by FG-SWCNTs

In this study, the nonlocal strain gradient theory is used because the structural dimensions are values between micrometer and nanometer. The viscoelastic property of the nanocomposite plate is also considered for vibration analysis of this system. The constitutive equations of FG-SWCNTs-reinforced porous nanocomposite viscoelastic and piezoelectric plate are as follows (Lim *et al.* 2015, Malikan *et al.* 2020, Malikan and Nguyen 2018, Malikan *et al.* 2018b)

$$\begin{cases} \left(1-(e_0a)^2\nabla^2\right)\sigma_{xx} = \left(1-\ell^2\nabla^2\right)\left(1+\tau_d\dfrac{\partial}{\partial t}\right)\left(Q_{11}\varepsilon_{xx}+Q_{12}\varepsilon_{yy}\right)-e_{31}E_z, \\ \left(1-(e_0a)^2\nabla^2\right)\sigma_{yy} = \left(1-\ell^2\nabla^2\right)\left(1+\tau_d\dfrac{\partial}{\partial t}\right)\left(Q_{12}\varepsilon_{xx}+Q_{22}\varepsilon_{yy}\right)-e_{32}E_z, \\ \left(1-(e_0a)^2\nabla^2\right)\tau_{xy} = \left(1-\ell^2\nabla^2\right)\left(1+\tau_d\dfrac{\partial}{\partial t}\right)Q_{66}\gamma_{xy}, \end{cases} \tag{8}$$

where ℓ, e_0a and τ_d are strain gradient parameter, nonlocal parameter and damping coefficient, respectively. (σ_{xx}, σ_{yy}), τ_{xy}, (ε_{xx}, ε_{yy}), γ_{xy}, E_z and e_{ij} are normal stresses, shear stress, normal strains, shear strain, electric field in z direction and piezoelectric coefficient, respectively. Also, Q_{ij} is elasticity parameters that is presented in Eq. (14).

Also for the piezoelectric property of this plate, the electric displacement-electric field relation is considered as follows (Mohammadimehr *et al.* 2016a, Ghorbanpour Arani *et al.* 2016)

$$\begin{cases}\left(1-\left(e_0a\right)^2\nabla^2\right)D_x=\left(1-\ell^2\nabla^2\right)\xi_{11}E_x,\\ \left(1-\left(e_0a\right)^2\nabla^2\right)D_y=\left(1-\ell^2\nabla^2\right)\xi_{22}E_y,\\ \left(1-\left(e_0a\right)^2\nabla^2\right)D_Z=\left(1-\ell^2\nabla^2\right)(e_{31}\varepsilon_{xx}+e_{32}\varepsilon_{yy}+\xi_{33}E_z),\end{cases} \tag{9}$$

in which D_i, E_i and ξ_{ij} are electric displacement, electric field, and dielectric coefficient, respectively. Due to Gholami and Ansari (2017), electric-field equations are as follows

$$\begin{cases}E=-\nabla\Phi,\\ \Phi=-\cos\left(\beta' z\right)\phi_E\left(x,y\right)+\dfrac{2z}{h}V_E,\end{cases} \tag{10}$$

$$\begin{cases}E_x=-\dfrac{\partial\Phi}{\partial x}=\cos\left(\beta' z\right)\dfrac{\partial\phi_E}{\partial x},\\ E_y=-\dfrac{\partial\Phi}{\partial y}=\cos\left(\beta' z\right)\dfrac{\partial\phi_E}{\partial y},\\ E_z=-\dfrac{\partial\Phi}{\partial y}=-\beta'\sin\left(\beta' z\right)\phi_E-\dfrac{2V_E}{h},\\ \beta'=\pi/h,\end{cases} \tag{11}$$

where Φ and V_E are electric potential and external electric voltage, respectively.

Eqs. (10), (11) can be expressed as follows

$$\begin{aligned}\left(1-\left(e_0a\right)^2\nabla^2\right)\begin{Bmatrix}\sigma_{xx}\\ \sigma_{yy}\\ \tau_{xy}\end{Bmatrix}&=\left(1-\ell^2\nabla^2\right)\left(1+\tau_d\frac{\partial}{\partial t}\right)\\ &\left(\begin{bmatrix}Q_{11}&Q_{12}&0\\ Q_{12}&Q_{22}&0\\ 0&0&Q_{66}\end{bmatrix}\begin{Bmatrix}\varepsilon_{xx}\\ \varepsilon_{yy}\\ \gamma_{xy}\end{Bmatrix}\right.\\ &\left.-\begin{bmatrix}0&0&e_{31}\\ 0&0&e_{32}\\ 0&0&0\end{bmatrix}\begin{Bmatrix}E_x\\ E_y\\ E_z\end{Bmatrix}\right),\end{aligned} \tag{12}$$

$$\begin{aligned}\left(1-\left(e_0a\right)^2\nabla^2\right)\begin{Bmatrix}D_x\\ D_y\\ D_z\end{Bmatrix}&=\left(1-\ell^2\nabla^2\right)\\ &\left(\begin{bmatrix}0&0&0\\ 0&0&0\\ e_{31}&e_{32}&0\end{bmatrix}\begin{Bmatrix}\varepsilon_{xx}\\ \varepsilon_{yy}\\ \gamma_{xy}\end{Bmatrix}+\begin{bmatrix}\xi_{11}&0&0\\ 0&\xi_{22}&0\\ 0&0&\xi_{33}\end{bmatrix}\begin{Bmatrix}E_x\\ E_y\\ E_z\end{Bmatrix}\right),\end{aligned} \tag{13}$$

$$\begin{cases}Q_{11}(z)=\dfrac{E_x(z)}{1-\upsilon_{12}\upsilon_{21}}, & Q_{12}(z)=\dfrac{\upsilon_{21}E_x(z)}{1-\upsilon_{12}\upsilon_{21}},\\ Q_{22}(z)=\dfrac{E_y(z)}{1-\upsilon_{12}\upsilon_{21}}, & Q_{66}(z)=E_{xy}(z),\end{cases} \tag{14}$$

in which e_{31}, e_{32}, ξ_{11}, ξ_{22} and ξ_{33} values are listed in Table 4 (Ghorbanpour Arani *et al.* 2016). Also, Q_{ij} is elasticity parameters and $E_x(z)$, $E_y(z)$ and $E_{xy}(z)$ are elasticity modulus of FG-SWCNTs-reinforced porous nanocomposite plate (Eq. (7)). Moreover, υ_{12} is Poisson's ratio which was defined in Eq. (5).

4.2 displacement fields and strain-displacement relations

The displacement fields for classical plate theory with Cartesian coordinates in x, y and z directions which can be represented by $u_1(x,y,z,t)$, $u_2(x,y,z,t)$ and $u_3(x,y,z,t)$ respectively, can be written as follows (Thai and Choi 2013)

$$\begin{cases}u_1(x,y,z,t)=u_0(x,y,t)-z\dfrac{\partial w(x,y,t)}{\partial x},\\ u_2(x,y,z,t)=v_0(x,y,t)-z\dfrac{\partial w(x,y,t)}{\partial y},\\ u_3(x,y,z,t)=w(x,y,t),\end{cases} \tag{15}$$

in which $u_0(x,y,t)$, $v_0(x,y,t)$ and $w(x,y,t)$ are the axial and transverse displacements of the mid-plane along the coordinate directions; while $u_1(x,y,z,t)$, $u_2(x,y,z,t)$ and $u_3(x,y,z,t)$ denote the axial and transverse displacements along the whole domain.

According to Eq. (15) the strain-displacement relations of the CPT are as follows (Thai and Choi 2013)

$$\begin{cases}\varepsilon_{xx}=\dfrac{\partial u_1}{\partial x}=\dfrac{\partial u_0}{\partial x}-z\dfrac{\partial^2 w}{\partial x^2},\\ \varepsilon_{yy}=\dfrac{\partial u_2}{\partial y}=\dfrac{\partial v_0}{\partial y}-z\dfrac{\partial^2 w}{\partial y^2},\\ \gamma_{xy}=\dfrac{\partial u_1}{\partial y}+\dfrac{\partial u_2}{\partial x}=\dfrac{\partial u_0}{\partial y}+\dfrac{\partial v_0}{\partial x}-2z\dfrac{\partial^2 w}{\partial x\,\partial y}.\end{cases} \tag{16}$$

4.3 Governing equations of motion

In this paper, energy method and Hamilton's principle are used to obtain governing equations of motion. In the energy method, the total potential energy $\prod$ is obtained from the strain energy U, kinetic energy K and energy due to the external loads Ω and is defined as follows (Mohammadimehr *et al.* 2016a, Ghorbanpour Arani *et al.* 2016)

$$\Pi=K-(U+\Omega), \tag{17}$$

$$\begin{cases}U=\dfrac{1}{2}\int_\forall(\sigma_{xx}\varepsilon_{xx}+\sigma_{yy}\varepsilon_{yy}+\tau_{xy}\gamma_{xy}-D_xE_x-D_yE_y-D_zE_z)d\forall,\\ K=\dfrac{1}{2}\int_\forall\rho_{(z)}(\dot{u}_1^2+\dot{u}_2^2+\dot{u}_3^2)d\forall,\\ \Omega=-\dfrac{1}{2}\int_0^b\int_0^a Fw\,dx\,dy,\end{cases} \tag{18}$$

$$F=N_{x_0}\left(\frac{\partial^2 w}{\partial x^2}\right)+N_{y_0}\left(\frac{\partial^2 w}{\partial y^2}\right)+q(x,y,t), \tag{19}$$

where $q(x,y,t)$ is transverse load per length and N_{x_0}, N_{y_0} are

biaxial forces. Also, *U*, *K*, and Ω are the strain energy, kinetic energy and energy due to the external loads, respectively. Rectangular plates are usually exposed to axial forces, so the tensions caused by this force and its effect on the frequency should be taken into account.

Considering Hamilton's principle Eq. (20) (Thai and Choi 2013), the Eq. (18) transforms into Eq. (21)

$$\delta\int_{t_1}^{t_2}\left(K-U-\Omega\right)dt \Rightarrow \int_{t_1}^{t_2}\left(\delta K-\left(\delta U+\delta\Omega\right)\right)dt=0, \quad (20)$$

$$\begin{cases} \delta U=\int_A\int_{-\frac{h}{2}}^{\frac{h}{2}}(\sigma_{xx}\delta\varepsilon_{xx}+\sigma_{yy}\delta\varepsilon_{yy}+\tau_{xy}\delta\gamma_{xy} \\ \quad -D_x\delta E_x-D_y\delta E_y-D_z\delta E_z)dzdA, \\ \delta K=\int_A\int_{-\frac{h}{2}}^{\frac{h}{2}}\rho_{(z)}(\frac{\partial}{\partial t}(u_1)\frac{\partial}{\partial t}(\delta u_1)+\frac{\partial}{\partial t}(u_2)\frac{\partial}{\partial t}(\delta u_2) \\ \quad +\frac{\partial}{\partial t}(u_3)\frac{\partial}{\partial t}(\delta u_3))dzdA, \\ \delta\Omega=-\int_0^b\int_0^a F\delta w dxdy. \end{cases} \quad (21)$$

Given the following assumptions (stress resultant), the equations of motion are obtained.

$$\begin{Bmatrix} N_x \\ N_y \\ N_{xy} \end{Bmatrix}=\int\begin{Bmatrix} \sigma_{xx} \\ \sigma_{yy} \\ \tau_{xy} \end{Bmatrix}dz,\ \begin{Bmatrix} M_x \\ M_y \\ M_{xy} \end{Bmatrix}=\int\begin{Bmatrix} \sigma_{xx} \\ \sigma_{yy} \\ \tau_{xy} \end{Bmatrix}zdz, \quad \begin{Bmatrix} \overline{D}_x \\ \overline{D}_y \\ \overline{D}_z \end{Bmatrix}=\int\begin{Bmatrix} D_x \\ D_y \\ D_z \end{Bmatrix}dz, \quad (22)$$

$$I^{(i)}=\int\rho_{(z)}z^{(i)}dz. \quad (23)$$

By inserting Eqs. (8), (9), (11), (22), (23) in the principle of Hamilton's Eq. (20) and finally, the four equations of motion are obtained by separating the coefficients for each independent variable and zeroing the δu, δv, δw and $\delta\phi_E$ coefficients.

$$\delta u: I^1\frac{\partial^3 w}{\partial x\,\partial t^2}-I^0\frac{\partial^2 u_0}{\partial t^2}+\frac{\partial N_x}{\partial x}+\frac{\partial N_{xy}}{\partial y}=0, \quad (24)$$

$$\delta v: I^1\frac{\partial^3 w}{\partial y\,\partial t^2}-I^0\frac{\partial^2 v_0}{\partial t^2}+\frac{\partial N_y}{\partial y}+\frac{\partial N_{xy}}{\partial x}=0, \quad (25)$$

$$\begin{cases} \delta w: I^2\frac{\partial^4 w}{\partial x^2\partial t^2}+I^2\frac{\partial^4 w}{\partial y^2\partial t^2}-I^1\frac{\partial^3 u_0}{\partial x\partial t^2} \\ \quad -I^1\frac{\partial^3 v_0}{\partial y\partial t^2}-I^0\frac{\partial^2 w}{\partial t^2} \\ +\frac{\partial^2 M_x}{\partial x^2}+\frac{\partial^2 M_y}{\partial y^2}+2\frac{\partial^2 M_{xy}}{\partial x\partial y}+N_{x_0}\left(\frac{\partial^2 w}{\partial x^2}\right) \\ \quad +N_{y_0}(\frac{\partial^2 w}{\partial y^2})+q(x,y,t)=0, \end{cases} \quad (26)$$

$$\delta\phi_E:\frac{\partial\overline{D}_x}{\partial x}+\frac{\partial\overline{D}_y}{\partial y}+\frac{\partial\overline{D}_z}{\partial z}=0. \quad (27)$$

In order to complete the governing equations of motion, first, by substituting strain-displacement Eq. (16) and electric-field Eq. (11) in the stress-strain Eq. (8), stress-displacement relations are obtained (see Eq. (28)).

Also by inserting strain-displacement Eq. (16) and electric-field Eq. (11) into Eq. (9), the electric displacement-electric field equation is completed (see Eq. (29)).

$$\begin{cases} \bullet\,(1-(e_0a)^2\nabla^2)\sigma_{xx}=\left(1-\ell^2\nabla^2\right)\left(1+\tau_d\frac{\partial}{\partial t}\right) \\ \left(\frac{E_{x_{(Z)}}}{1-\upsilon^2}\left(\frac{\partial u_0}{\partial x}-z\frac{\partial^2 w}{\partial x^2}\right)+\frac{\upsilon E_{x_{(Z)}}}{1-\upsilon^2}\left(\frac{\partial v_0}{\partial y}-z\frac{\partial^2 w}{\partial y^2}\right)\right) \\ -e_{31}\left(-\beta' sin(\beta' z)\,\phi_E-\frac{2V_E}{h}\right), \\ \bullet\,(1-(e_0a)^2\nabla^2)\sigma_{yy}=\left(1-\ell^2\nabla^2\right) \\ \left(1+\tau_d\frac{\partial}{\partial t}\right)\left(\frac{\upsilon E_{x_{(Z)}}}{1-\upsilon^2}\left(\frac{\partial u_0}{\partial x}-z\frac{\partial^2 w}{\partial x^2}\right)+\frac{E_{y_{(Z)}}}{1-\upsilon^2}\left(\frac{\partial v_0}{\partial y}-z\frac{\partial^2 w}{\partial y^2}\right)\right) \\ -e_{32}\left(-\beta' sin(\beta' z)\,\phi_E-\frac{2V_E}{h}\right), \\ \bullet\,(1-(e_0a)^2\nabla^2)\tau_{xy}=\left(1-\ell^2\nabla^2\right) \\ \left(1+\tau_d\frac{\partial}{\partial t}\right)E_{xy_{(Z)}}\left(\frac{\partial u_0}{\partial y}+\frac{\partial v_0}{\partial x}-2z\frac{\partial^2 w}{\partial x\partial y}\right), \end{cases} \quad (28)$$

$$\begin{cases} (1-(e_0a)^2\nabla^2)D_x=\left(1-\ell^2\nabla^2\right)\xi_{11}\left(cos(\beta' z)\frac{\partial\phi_E}{\partial x}\right), \\ (1-(e_0a)^2\nabla^2)D_y=\left(1-\ell^2\nabla^2\right)\xi_{22}\left(cos(\beta' z)\frac{\partial\phi_E}{\partial y}\right), \\ (1-(e_0a)^2\nabla^2)D_Z=\left(1-\ell^2\nabla^2\right)(e_{31}\left(\frac{\partial u_0}{\partial x}-z\frac{\partial^2 w}{\partial x^2}\right) \\ \quad +e_{32}\left(\frac{\partial v_0}{\partial y}-z\frac{\partial^2 w}{\partial y^2}\right) \\ +\xi_{33}\left(-\beta' sin(\beta' z)\,\phi_E-\frac{2V_E}{h}\right)). \end{cases} \quad (29)$$

Now by using following assumptions (Eq. (30)) into Eqs. (28), (29) and replacing them into Eq. (22), stress resultants are obtained which are given in Appendix A

$$\begin{aligned} A_x^{(i)}&=\int E_{x_{(z)}}z^{(i)}dz, \\ A_y^{(i)}&=\int E_{y_{(z)}}z^{(i)}dz, \\ A_{xy}^{(i)}&=\int E_{xy_{(z)}}z^{(i)}dz, \\ B^{(i)}&=\int z^{(i)}dz, \\ C^{(i)}&=\int z^{(i)}\sin\left(\beta' z\right)dz, \\ D^{(i)}&=\int z^{(i)}\cos\left(\beta' z\right)dz,\ \ i=0,1,2. \end{aligned} \quad (30)$$

Finally, the governing equations of motion are completed by substituting the equations of Appendix A in Eqs. (24)-(27).

5. Analytical solutions

Vibration solutions for a simply supported rectangular

FG-SWCNTs-reinforced plate under a transverse load $q(x,y,t)$ and superficial (axial) forces: $N_{x_0}=\gamma_1 N_{cr}$, $N_{y_0}=\gamma_2 N_{cr}$ and $N_{xy_0}=0$, have been solved through Navier's approach. This solution satisfies the equations of motion and boundary conditions by the following relations (Thai and Choi 2013)

$$\begin{cases} u(x,y,t)=\sum_{m=1}^{\infty}\sum_{n=1}^{\infty}U_{mn}\cos\alpha x\,\sin\beta y\;e^{i\omega t}, \\ v(x,y,t)=\sum_{m=1}^{\infty}\sum_{n=1}^{\infty}V_{mn}\sin\alpha x\,\cos\beta y\;e^{i\omega t}, \\ w(x,y,t)=\sum_{m=1}^{\infty}\sum_{n=1}^{\infty}W_{mn}\sin\alpha x\,\sin\beta y\;e^{i\omega t}, \\ \phi_E(x,y,t)=\sum_{m=1}^{\infty}\sum_{n=1}^{\infty}\Phi_{mn}\sin\alpha x\,\sin\beta y\,e^{i\omega t}, \end{cases} \tag{31a}$$

where ω is frequency, $i=\sqrt{-1}$, $\alpha=m\frac{\pi}{a}$, $\beta=m\frac{\pi}{b}$ and $\{U_{mn}, V_{mn}, W_{mn}, \Phi_{mn}\}$are coefficients.

According to Mohammadimehr *et al.* (2018b) for closed-circuit boundary conditions of piezoelectric materials, we have

$$\begin{aligned} &\phi_E(x=0,y,t)=0, \\ &\phi_E(x=a,y,t)=0, \\ &\phi_E(x,y=0,t)=0, \\ &\phi_E(x,y=b,t)=0. \end{aligned} \tag{31b}$$

Thus, based on the closed-circuit boundary conditions, the relation (31a) is suggested that is satisfied the electric boundary conditions.

Substitute Eq. (31a) into the equations of motion, the analytical solutions of the CPT can be acquired from the following equations

$$\begin{Bmatrix} \frac{\partial x}{\partial t} \\ \frac{\partial^2 x}{\partial t^2} \end{Bmatrix}=\begin{bmatrix} [0] & [I] \\ -[M^{-1}][K] & -[M^{-1}][C] \end{bmatrix}\begin{Bmatrix} y \\ \frac{\partial y}{\partial t} \end{Bmatrix}, \tag{32}$$

$$K=\begin{bmatrix} k_{11} & k_{12} & k_{13} & k_{14} \\ k_{21} & k_{22} & k_{23} & k_{24} \\ k_{31} & k_{32} & k_{33} & k_{34} \\ k_{41} & k_{42} & k_{43} & k_{44} \end{bmatrix},$$

$$C=\begin{bmatrix} c_{11} & c_{12} & c_{13} & c_{14} \\ c_{21} & c_{22} & c_{23} & c_{24} \\ c_{31} & c_{32} & c_{33} & c_{34} \\ c_{41} & c_{42} & c_{43} & c_{44} \end{bmatrix}, \tag{33}$$

$$M=\begin{bmatrix} m_{11} & m_{12} & m_{13} & m_{14} \\ m_{21} & m_{22} & m_{23} & m_{24} \\ m_{31} & m_{32} & m_{33} & m_{34} \\ m_{41} & m_{42} & m_{43} & m_{44} \end{bmatrix},$$

where K is the stiffness matrix, C is the damping matrix, and M is the mass matrix. The entries of these matrices are shown in Appendix B.

Table 4 Piezoelectric properties of PVDF (Ghorbanpour Arani *et al.* 2016)

e_{31} (C/m^2)	e_{32} (C/m^2)	ξ_{11} (F/m)	ξ_{22} (F/m)	ξ_{33} (F/m)
-0.13	-0.145	1.1068e-8	1.1067e-8	1.1067e-8

Table 5 Comparison of nondimensional natural frequency of a homogenous simply supported square plate with various values of aspect ratio

$\overline{\omega}$	a/h	Thai and Choi 2013	Present work	Diff (%)
Fundamental natural frequency	5	5.9671	5.9671	0
	10	6.1103	6.1103	0
	20	6.1477	6.1477	0
Second natural frequency	5	14.2717	14.2717	0
	10	15.0936	15.0936	0
	20	15.3223	15.3223	0

6. Numerical results and discussion

Table 4 shows the piezoelectric properties of PVDF presented by Ghorbanpour Arani *et al.* (2016). Before investigating the numerical results of the vibration analysis, results validation is necessary. First of all the porosity coefficient is assumed zero (homogeneous plate e=0) due to unavailability of the FG-SWCNTs-reinforced microplate results in this article. Tabulated results are summarized in Table 5 which illustrates the comparison of non-dimensional natural frequencies with those reported by Thai and Choi 2013 for a homogenous simply supported square plate. This comparison indicates that present work is consistent with the results of Thai and Choi (2013) with following properties (Thai and Choi 2013, Rezaei and Saidi 2015)

$$\begin{cases} E_{(z)}=E_0\left(1\text{-}e\cos\left(\frac{\pi}{2\hbar}(z+\frac{\hbar}{2})\right)\right), \\ \rho_{(z)}=\rho_0\left(1\text{-}e'\cos\left(\frac{\pi}{2\hbar}(z+\frac{\hbar}{2})\right)\right), \\ e'=1-\sqrt{1-e}, \end{cases} \tag{34}$$

$$\begin{cases} E_0=14.4GPa, & e=0, \quad a=b, \quad \ell=0, \\ E_1=1.44GPa, & q_0=1N, \quad \hbar=17.6\times10^{-6}m, \\ \rho_0=12200\frac{Kg}{m^3}, & \rho_1=1220\frac{Kg}{m^3}, \quad \nu=0.38. \end{cases} \tag{35}$$

Since this case isn't piezoelectric and it's without damping coefficient, the analytical solutions of the CPT can be obtained from the following equation (Mohammadimehr *et al.* 2016b)

$$\left(\begin{bmatrix} k_{11} & k_{12} & k_{13} \\ k_{21} & k_{22} & k_{23} \\ k_{31} & k_{32} & k_{33} \end{bmatrix}-\omega^2\begin{bmatrix} m_{11} & m_{12} & m_{13} \\ m_{21} & m_{22} & m_{23} \\ m_{31} & m_{32} & m_{33} \end{bmatrix}\right)$$

Table 6 Natural frequency ω of a simply supported FG-SWCNTs-reinforced plate with various values of porosity coefficient (10^7 rad/s)

Fundamental natural frequency a/h	ℓ/h	e=0	e=0.2	e=0.5	e=0.9
10	0	3.7377	3.6295	3.4072	2.7468
	0.2	3.7524	3.6438	3.4206	2.7577
	0.5	3.8288	3.7180	3.4902	2.8138
	0.8	3.9668	3.8519	3.6160	2.9152
	1	4.0900	3.9716	3.7283	3.0057
20	0	1.0995	1.0635	1.0065	0.9562
	0.2	1.1006	1.0645	1.0075	0.9571
	0.5	1.1063	1.0700	1.0127	0.9621
	0.8	1.1168	1.0802	1.0223	0.9712
	1	1.1263	1.0894	1.0310	0.9795
30	0	0.7330	0.7090	0.6710	0.6374
	0.2	0.7333	0.7093	0.6713	0.6378
	0.5	0.7350	0.7195	0.6728	0.6392
	0.8	0.7381	0.7140	0.6757	0.6420
	1	0.7410	0.7167	0.6783	0.6444
40	0	0.5498	0.5317	0.5032	0.4781
	0.2	0.5499	0.5319	0.5034	0.4782
	0.5	0.5506	0.5326	0.5040	0.4788
	0.8	0.5519	0.5338	0.5052	0.4800
	1	0.5531	0.5350	0.5063	0.4810
Second natural frequency a/h	ℓ/h	e=0	e=0.2	e=0.5	e=0.9
10	0	6.5629	6.3479	6.0080	5.7099
	0.2	6.6273	6.4103	6.0670	5.7660
	0.5	6.9560	6.7281	6.3678	6.0519
	0.8	7.5282	7.2817	6.8917	6.5498
	1	8.0203	7.7577	7.3423	6.9780
20	0	3.2814	3.1739	3.0039	2.8540
	0.2	3.2895	3.1818	3.0113	2.8611
	0.5	3.3316	3.2225	3.0498	2.8977
	0.8	3.4085	3.2969	3.1202	2.9646
	1	3.4780	3.3640	3.1838	3.0250
30	0	2.1876	2.1160	2.0025	1.9025
	0.2	2.1900	2.1183	2.0047	1.9046
	0.5	2.2026	2.1304	2.0162	1.9115
	0.8	2.2257	2.1528	2.0374	1.9356
	1	2.2468	2.1732	2.0567	1.95400
40	0	1.6407	1.5870	1.5020	1.4268
	0.2	1.6417	1.5879	1.5028	1.4277
	0.5	1.6470	1.5931	1.5077	1.4323
	0.8	1.6568	1.6025	1.5166	1.4409
	1	1.6658	1.6112	1.5249	1.4487

$$\begin{Bmatrix} U_{mn} \\ V_{mn} \\ W_{mn} \end{Bmatrix} = \begin{Bmatrix} 0 \\ 0 \\ Q_{mn} \end{Bmatrix}. \tag{36}$$

The nondimensional frequency $\bar{\omega}$ is acquired from following equations (Thai and Choi 2013)

$$\bar{\omega} = \omega\left(\frac{a^2}{h}\right)\sqrt{\frac{\rho_1}{E_1}}. \tag{37}$$

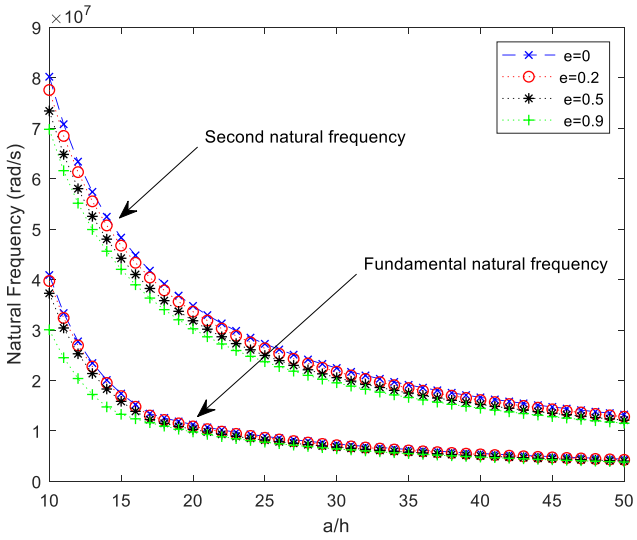

Fig. 3 Effect of porosity coefficient on the fundamental and second natural frequency of a simply supported FG-SWCNTs-reinforced plate with ℓ/h

6.1 Vibration analysis of the FG-SWCNTs-reinforced porous nanocomposite viscoelastic and piezoelectric rectangular plate

Assume a simply supported square FG-SWCNTs-reinforced plate with the following material properties

$$\begin{cases} h = 34 \ \ nm, \quad T = 300 \ \ K, \quad q_0 = 1000 \ \ N, \\ e_0 a = 0.5 \ \ nm, \quad \Delta T = 25, \quad \ell = h, \\ \tau_d = 0.01, \ \ V^*_{CNT} = 0.11, \\ a = b, \ e = 0, \ 0.2, \ 0.5, \ 0.9. \end{cases} \tag{38}$$

In Table 6, fundamental and second natural frequency of the porous nanocomposite viscoelastic and piezoelectric plate reinforced by FG-SWCNTs are tabulated with various values of porosity coefficient for different strain gradient parameter and aspect ratio values. It is observed that with increasing porosity and aspect ratio, natural frequency decreases and by increasing strain gradient parameter, natural frequency increases.

The effect of porosity coefficient with respect to aspect ratio a/h on the dimensional and nondimensional natural frequency of a simply supported FG-SWCNTs-reinforced plate is shown in Figs. 3 and 4, respectively. It is also depicted from these figures, as porosity coefficient increases, stiffness of porous nanocomposite plate reduces and therefore dimensional and nondimensional natural frequency decrease. It is seen from Figs. 3 and 4 that with increasing of porosity coefficient, the nanocomposite plate becomes softer. Also, by increasing the value of aspect ratio, dimensional natural frequency decreases and nondimensional natural frequency increases. The physical reason for the break in results of fundamental natural frequency in Fig. 4 is that for lower aspect ratio (a/h<17), it is better to use first order shear deformation theory and for higher aspect ratio (a/h>=17), the results for classical plate theory is good; while we consider for all ranges classical plate theory.

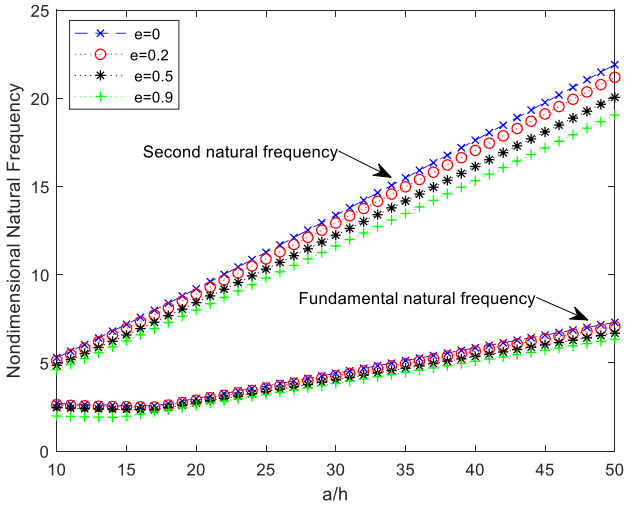

Fig. 4 Effect of porosity coefficient on the nondimensional fundamental and second natural frequency of a simply supported FG-SWCNTs-reinforced plate with ℓ/h

Table 7 Natural frequency ω of a simply supported FG-SWCNTs-reinforced plate with various values nonlocal parameter with h=20 nm and e=0.5 (10^8 rad/s)

Fundamental natural frequency / a/h	ℓ/h	e_0a=0	e_0a=0.5 nm	e_0a=1 nm	e_0a=1.5 nm	e_0a=2 nm
10	0	5.7922	5.7919	5.7908	5.7890	5.7865
	0.5	5.9334	5.1933	5.9320	5.9301	5.9276
	1	6.3382	6.3378	6.3366	6.3347	6.3319
20	0	1.7110	1.7110	1.7109	1.7108	1.7106
	0.5	1.7216	1.7215	1.7215	1.7213	1.7211
	1	1.7528	1.7527	1.7526	1.7525	1.7523
30	0	1.1407	1.1407	1.1407	1.1406	1.1406
	0.5	1.1438	1.1438	1.1438	1.1437	1.1437
	1	1.1531	1.1531	1.1531	1.1531	1.1531
40	0	0.8555	0.8555	0.8555	0.8555	0.8555
	0.5	0.8568	0.8568	0.8568	0.8568	0.8568
	1	0.8608	0.8608	0.8608	0.8607	0.8607
Second natural frequency / a/h	ℓ/h	e_0a=0	e_0a=0.5 nm	e_0a=1 nm	e_0a=1.5 nm	e_0a=2 nm
10	0	10.2136	10.2120	10.2073	10.1994	10.1884
	0.5	10.8253	10.8236	10.8186	10.8103	10.7986
	1	12.4818	12.4799	12.4741	12.4645	12.4510
20	0	5.1066	5.1064	5.1058	5.1048	5.1034
	0.5	5.1847	5.1845	5.1839	5.1829	5.1815
	1	5.4124	5.4122	5.4116	5.4105	5.4091
30	0	3.4043	3.4043	3.4041	3.4038	3.4034
	0.5	3.4276	3.4275	3.4273	3.4270	3.4266
	1	3.4964	3.4963	3.4961	3.4959	3.4954
40	0	2.5532	2.5532	2.5531	2.5530	2.5528
	0.5	2.5630	2.5630	2.5630	2.5628	2.5627
	1	2.5923	2.5923	2.5922	2.5921	2.5919

In Table 7 fundamental and second natural frequency are presented with various values of nonlocal parameter for different strain gradient parameter and aspect ratio values. It is observed from Table 7 that natural frequency decreases with an increase in nonlocal parameter and aspect ratio, and also it increases by increasing strain gradient parameter.

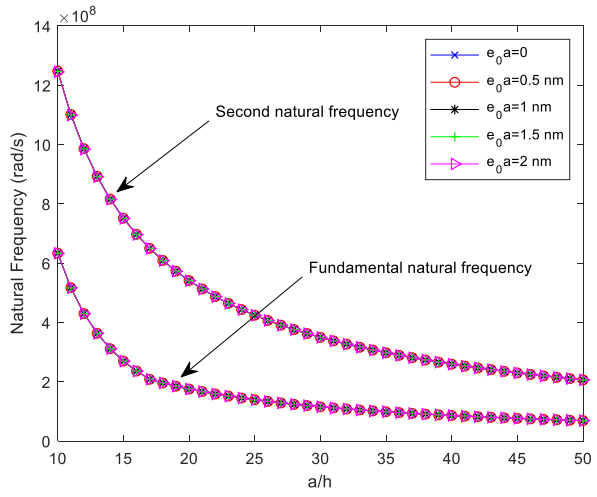

(a)

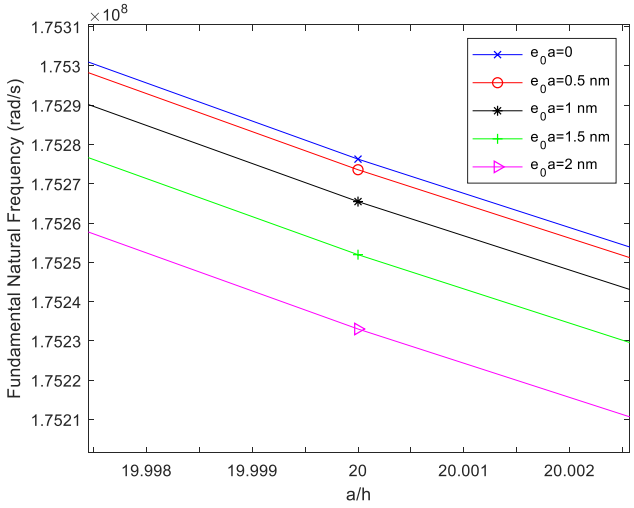

(b)

Fig. 5 Effect of nonlocal parameter on natural frequency of a simply supported FG-SWCNTs-reinforced plate with h=20 nm, ℓ/h and e=0.5: (a) fundamental and second natural frequency (b) fundamental natural frequency

Fig. 5 (a) indicates the effect of nonlocal parameter on the natural frequency (fundamental and second natural frequency) of a simply supported square plate reinforced by FG-SWCNTs with h=20 nm, ℓ/h and e=0.5. It can be seen that natural frequency decreases with an increase in nonlocal parameter and aspect ratio (see Fig. 5(b)), the physical reason is that the nanocomposite plate becomes softer with increasing of nonlocal parameter.

Figs. 6-9 illustrate the effects of strain gradient parameter ℓ (for different porosity coefficients and a=30h), damping coefficient τ_d, volume fraction of CNTs and temperature T on the fundamental natural frequency, respectively. It is concluded from Fig. 6 that when l/h is equal to zero, there is no strain gradient parameter, thus in this case, the structure is softer than when this ratio is not equal to zero ($l/h\neq0$). On the other hands, considering strain gradient parameter leads to increase the stiffness of nano strcucture. With regards to these figures, natural frequency

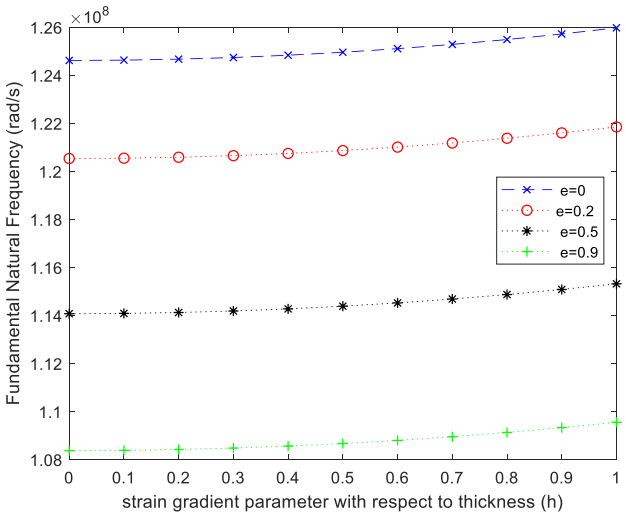

Fig. 6 Effect of strain gradient parameter ℓ on the fundamental natural frequency of a simply supported FG-SWCNTs-reinforced plate for different porosity coefficients with h=20 nm and a=30h

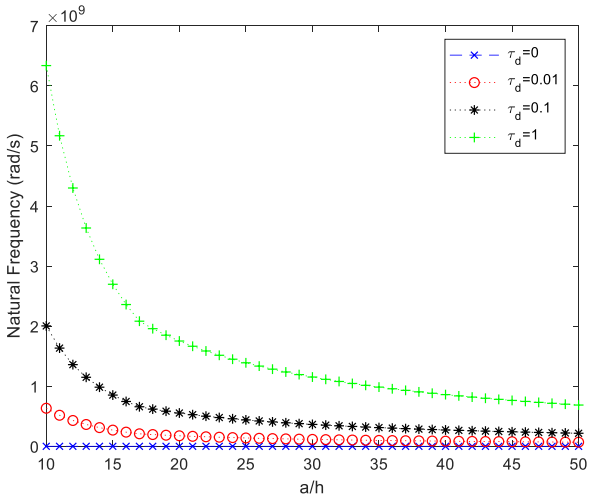

(a)

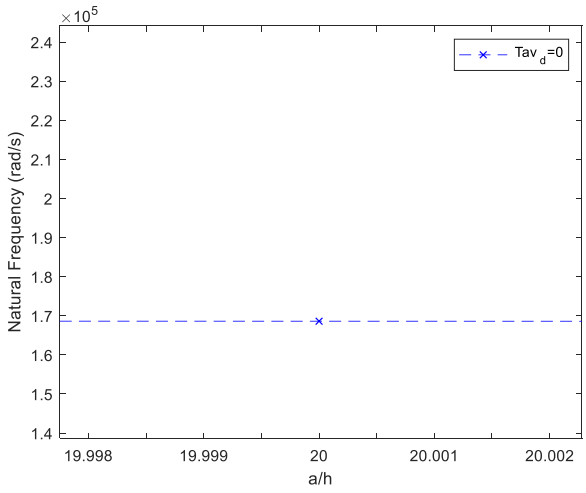

(b)

Fig. 7 Effect of damping coefficient τ_d on the fundamental natural frequency of a simply supported FG-SWCNTs-reinforced plate with h=20 nm, ℓ=h and e=0.5: (a) for various values of τ_d (b) for τ_d=0

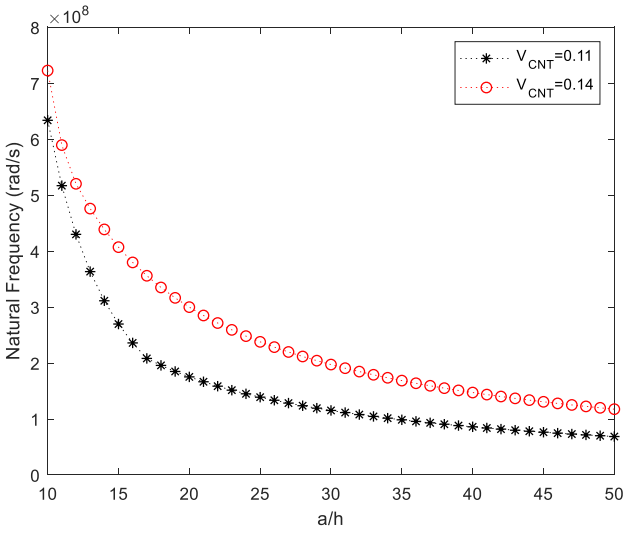

Fig. 8 Effect of CNTs volume fraction V_{CNT} on the fundamental natural frequency of a simply supported FG-SWCNTs-reinforced plate with h=20 nm, ℓ=h and e=0.5

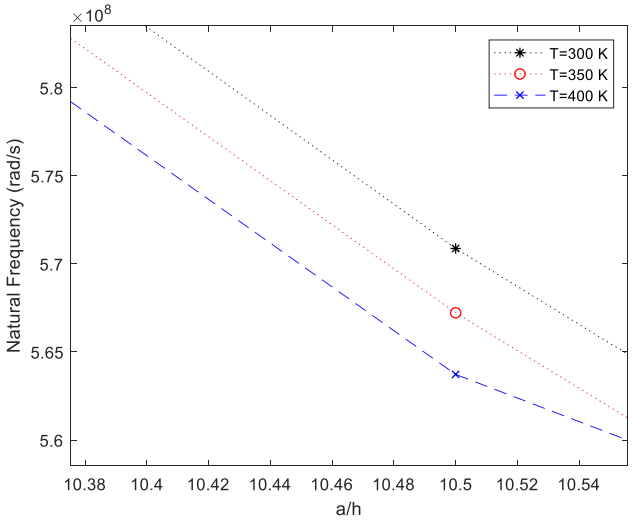

Fig. 9 Effect of temperature T on the fundamental natural frequency of a simply supported FG-SWCNTs-reinforced plate with h=20 nm, ℓ=h and e=0.5

decreases by increasing temperature (due to stiffness reduction) and increases by increasing volume fraction of CNTs (due to stiffness increase), strain gradient parameter and damping coefficient. Moreover, by increasing aspect ratio natural frequency decreases for the specified values of damping coefficient, volume fraction of CNTs and temperature (see Figs. 7-9). When the viscoelasticity is ignored, it is seem that the natural frequency is zero, thus to provide from the mistake, the authors zoom the Fig. 7(a), and then plot Fig. 7(b) for τ_d=0. It is seen that for τ_d=0, the natural frequency is equal 1.7×10^5 that for different values of τ_d =0.01, 0.1, 1 that range of natural frequency becomes between 0.8×10^9 to 6.5×10^9, thus the order τ_d=0 is 10^5; while for other value of τ_d, it is 10^9. Thus, when we plot different values of τ_d =0,0.01,0.1,1, it is seem for τ_d =0, that the naural frequency is equal to zero; while the value of natural frequency is 1.7×10^5. It is seen from Fig. 8 that with

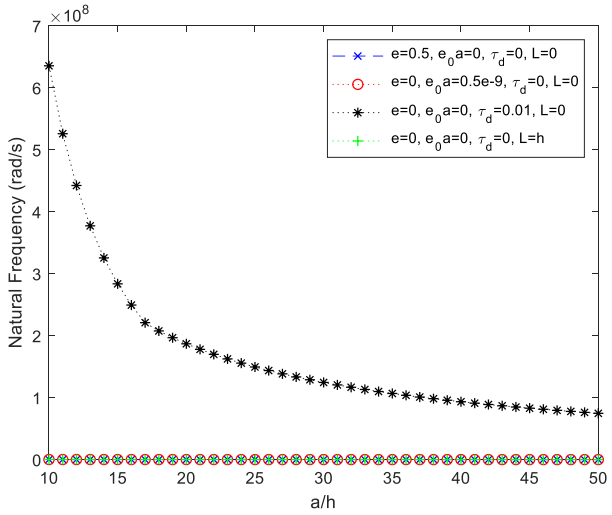

(a)

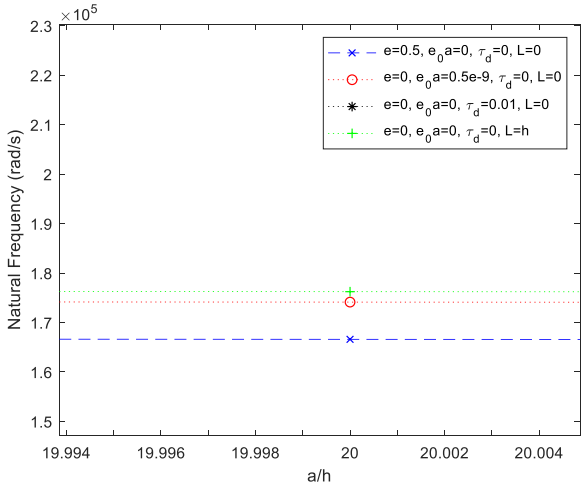

(b)

Fig. 10 Effectiveness rate of damping coefficient, strain gradient parameter, nonlocal parameter and porosity coefficient on the fundamental natural frequency of a simply supported FG-SWCNTs-reinforced plate with h=20 nm: (a) for $10<\frac{a}{h}<50$ (b) for $19.994<\frac{a}{h}<20.004$

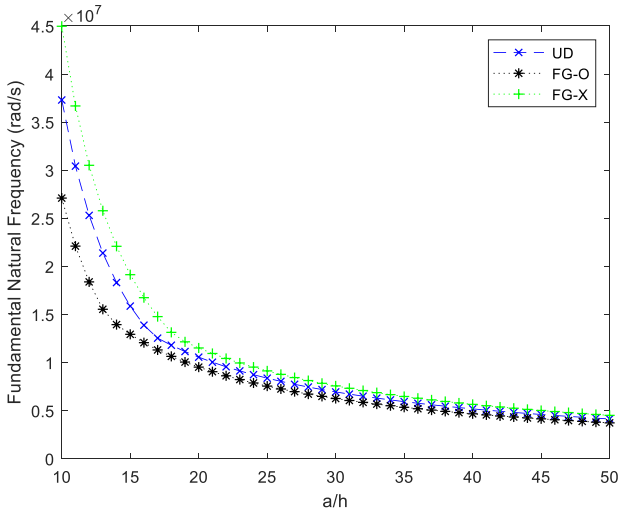

(a)

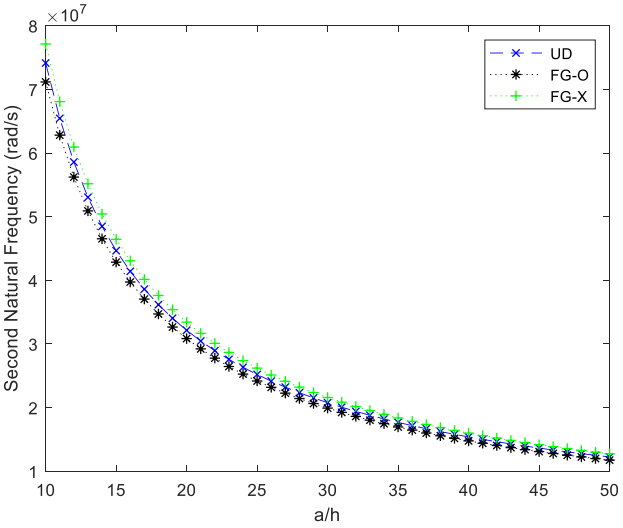

(b)

Fig. 11 Effect of various FG-SWCNTs distribution patterns (UD, FG-X and FG-O) on the natural frequency of a simply supported FG-SWCNTs-reinforced plate with h=340 nm, ℓ=h and e=0.5 (a) for fundamental natural frequency (b) for second natural frequency

an increase in the volume fraction of CNT, the natural frequency increases, the physical reason is that the nanocomposite plate becomes stiffer with increasing of volume fraction of CNT. It is shown from Fig. 9 that an increase in the temperature leads to decrease natural frequency due to reducing stiffness of nanocomposite plate. The physical reason for the break in results of fundamental natural frequency in Fig. 9 is that for higher temperature (T=400 K), the nanocomposite (specially polymer resin) cannot tolerate this temperature.

The effect of damping coefficient on the rise of the natural frequency is considerably more than the other parameters effect, and the strain gradient parameter, the nonlocal parameter and porosity coefficient have a lower effect on the natural frequency rise than the damping coefficient, respectively (See Fig. 10).

The Effect of various FG-SWCNTs distribution patterns (UD, FG-X and FG-O) on the fundamental and second natural frequency is shown in Fig. 11. The graphs show that for both fundamental and second natural frequency, FG-X distribution pattern have greater effects on the natural frequency than the other distributions. In addition, UD and FG-O, respectively, have lower effects than the FG-X on the natural frequency. It is seen from Fig. 11 that FG-X distribution results due to the strengthening of the edges leads to increase the stiffness nanocomposite plate, which has farthest from the mid-plane. Thus, the natural frequency increases, the physical reason is that the nanocomposite plate becomes stiffer with FG-X distribution of CNT.

7. Conclusions

This article considering the nonlocal strain gradient

theory, perused the size dependent effect on natural frequencies of a FG-SWCNTs reinforced viscoelastic and piezoelectric porous nanocomposite plate. The results reveal that the effect of damping coefficient on the increase of the natural frequency is greatly higher than the other parameters effect, and the strain gradient parameter and the nonlocal parameter have a lower effect on the natural frequency increase than the damping coefficient, respectively. Moreover, it can be comprehended from results that by increasing porosity or temperature, stiffness of the nanocomposite structure decreases and as a result natural frequency decreases and vice versa for increasing volume fraction. Further, natural frequency decreases with a raise in the nonlocal parameter and aspect ratio while it increases with increasing of strain gradient parameter and damping coefficient. By studying the different distribution patterns of FG-SWCNTs, one can see that the FG-O distribution produces less vibration than other distributions, so that in designs which need to reduce vibrations, this distribution will be appropriate. Also UD and FG-X, respectively, have greater effects on the natural frequency than the FG-O. This study can be used to optimize the industrial designs due to study the effects of various properties on the vibrations of the mentioned nanocomposite plates, one can reduce the vibrations of the desired structure, which is a very important issue in the optimizing designs of the automotive industry and aerospace engineering.

Acknowledgement

The authors would like to thank the referees for their valuable comments. Also, they are thankful to the Iranian Nanotechnology Development Committee for their financial support and the University of Kashan for supporting this work by Grant No. 891238/3.

References

Addou, F.Y., Meradjah, M., Bousahla, A.A., Benachour, A., Bourada, F., Tounsi, A. and Mahmoud, S.R. (2019), "Influences of porosity on dynamic response of FG plates resting on Winkler/Pasternak/Kerr foundation using quasi 3D HSDT", *Comput. Concrete*, **24**(4), 347-367. https://doi.org/10.12989/cac.2019.24.4.347.

Akbarzadeh Khorshidi, M. (2018), "The material length scale parameter used in couple stress theories is not a material constant", *Int. J. Eng. Sci.*, **133**, 15-25. https://doi.org/10.1016/j.ijengsci.2018.08.005.

AkhavanAlavi, S.M, Mohammadimehr, M. and Edjtahed, S.H. (2019), "Active control of micro Reddy beam integrated with functionally graded nanocomposite sensor and actuator based on linear quadratic regulator method", *Eur. J. Mech. A/Solid.*, **74**, 449-461. https://doi.org/10.1016/j.euromechsol.2018.12.008

Alibeigloo, A. (2013), "Static analysis of functionally graded carbon nanotube-reinforced composite plate embedded in piezoelectric layers by using theory of elasticity", *Compos. Struct.*, **95**, 612-622. https://doi.org/10.1016/j.compstruct.2012.08.018.

Amir, S., Soleimani-Javid, Z. and Arshid, E. (2019), "Size-dependent free vibration of sandwich micro beam with porous core subjected to thermal load based on SSDBT", *Z. Angew. Math. Mech.*, **99**(9), e201800334. https://doi.org/10.1002/zamm.201800334.

Ansari, R., Faghih-Shojaei, M., Mohammadi, V., Gholami, R. and Rouhi, H. (2015), "Buckling and postbuckling of single-walled carbon nanotubes based on a nonlocal Timoshenko beam model", *Z. Angew. Math. Mech.*, **95**(9), 939-951. https://doi.org/10.1002/zamm.201300017.

Arefi, M., Kiani, M. and Rabczuk, T. (2019), "Application of nonlocal strain gradient theory to size dependent bending analysis of a sandwich porous nanoplate integrated with piezomagnetic face-sheets", *Compos. Part. B. Eng.*, **168**, 320-333. https://doi.org/10.1016/j.compositesb.2019.02.057.

Arefi, M., Pourjamshidian, M. and Ghorbanpour-Arani, A. (2018), "Free vibration analysis of a piezoelectric curved sandwich nanobeam with FG-CNTRCs face-sheets based on various high-order shear deformation and nonlocal elasticity theories", *Eur. Phys. J. Plus.*, **133**(5), 193. https://doi.org/10.1140/epjp/i2018-12015-1.

Bousahla, A.A., Bourada, F., Mahmoud, S.R., Tounsi, A., Algarni, A., Bedia, E.A. and Tounsi, A. (2020), "Buckling and dynamic behavior of the simply supported CNT-RC beams using an integral-first shear deformation theory", *Comput. Concrete*, **25**(2), 155-166. https://doi.org/10.12989/cac.2020.25.2.155.

Dinh Duc, N., Quang, V.D., Nguyen, P.D. and Chien, T.M. (2018), "Nonlinear dynamic response of functionally graded porous plates on elastic foundation subjected to thermal and mechanical loads", *J. Appl. Comput. Mech.*, **4**(4), 245-259. https://dx.doi.org/10.22055/jacm.2018.23219.1151.

Ebrahimi, F. and Barati, M.R. (2017), "Porosity-dependent vibration analysis of piezo-magnetically actuated heterogeneous nanobeams", *Mech. Syst. Signal Pr.*, **93**, 445-459. https://doi.org/10.1016/j.ymssp.2017.02.021.

Ebrahimi, F. and Barati, M.R. (2018), "Damping vibration analysis of graphene sheets on viscoelastic medium incorporating hygro-thermal effects employing nonlocal strain gradient theory", *Compos. Struct.*, **185**, 241-253. https://doi.org/10.1016/j.compstruct.2017.10.021.

Ebrahimi, F. and Dabbagh, A. (2017), "Wave propagation analysis of embedded nanoplates based on a nonlocal strain gradient-based surface piezoelectricity theory", *Eur. Phys. J. Plus.*, **132**(11), 449. https://doi.org/10.1140/epjp/i2017-11694-2.

Ebrahimi, F. and Dabbagh, A. (2019), "An analytical solution for static stability of multi-scale hybrid nanocomposite plates", *Eng. Comput.*, 1-15. https://doi.org/10.1007/s00366-019-00840-y.

Ebrahimi, F. and Farazmandnia, N. (2017), "Thermo-mechanical vibration analysis of sandwich beams with functionally graded carbon nanotube-reinforced composite face sheets based on a higher-order shear deformation beam theory", *Mech. Adv. Mater. Struct.*, **24**(10), 820-829. https://doi.org/10.1080/15376494.2016.1196786.

Ebrahimi, F. and Shafiei, N. (2017), "Influence of initial shear stress on the vibration behavior of single-layered graphene sheets embedded in an elastic medium based on Reddy's higher-order shear deformation plate theory", *Mech. Adv. Mater. Struct.*, **24**(9), 761-772. https://doi.org/10.1080/15376494.2016.1196781.

Ebrahimi, F., Barati, M.R. and Civalek, Ö. (2019a), "Application of Chebyshev–Ritz method for static stability and vibration analysis of nonlocal microstructure-dependent nanostructures", *Eng. Comput.*, 1-12. https://doi.org/10.1007/s00366-019-00742-z.

Ebrahimi, F., Habibi, M. and Safarpour, H. (2019b), "On modeling of wave propagation in a thermally affected GNP-reinforced imperfect nanocomposite shell", *Eng. Comput.*, **35**(4), 1375-1389. https://doi.org/10.1007/s00366-018-0669-4.

Ebrahimi, F., Nouraei, M. and Dabbagh, A. (2019c), "Thermal vibration analysis of embedded graphene oxide powder-reinforced nanocomposite plates", *Eng. Comput.*, 1-17. https://doi.org/10.1007/s00366-019-00737-w.

Gao, Y., Xiao, W.S. and Zhu, H. (2019), "Nonlinear vibration

analysis of different types of functionally graded beams using nonlocal strain gradient theory and a two-step perturbation method", *Eur. Phys. J. Plus.*, **134**(1), 23. https://doi.org/10.1140/epjp/i2019-12446-0.

Gholami, R. and Ansari, R. (2017), "A unified nonlocal nonlinear higher-order shear deformable plate model for postbuckling analysis of piezoelectric-piezomagnetic rectangular nanoplates with various edge supports", *Compos. Struct.*, **166**, 202-218. https://doi.org/10.1016/j.compstruct.2017.01.045.

Ghorbanpour-Arani, A. and Jalaei, M.H. (2017), "Investigation of the longitudinal magnetic field effect on dynamic response of viscoelastic graphene sheet based on sinusoidal shear deformation theory", *Physica B*, **506**, 94-104. https://doi.org/10.1016/j.physb.2016.11.004.

Ghorbanpour-Arani, A., Jamali, M., Mosayyebi, M. and Kolahchi, R. (2016), "Wave propagation in FG-CNT-reinforced piezoelectric composite micro plates using viscoelastic quasi-3D sinusoidal shear deformation theory", *Compos. Part B. Eng.*, **95**, 209-224. https://doi.org/10.1016/j.compositesb.2016.03.077.

Ghorbanpour Arani, A., Rousta Navi, B. and Mohammadimehr, M. (2016), "Surface stress and agglomeration effects on nonlocal biaxial buckling polymeric nanocomposite plate reinforced by CNT using various approaches", *Adv. Compos. Mater.*, **25**(5), 423-441. https://doi.org/10.1080/09243046.2015.1052189.

Jafarian Arani, A. and Kolahchi, R. (2016), "Buckling analysis of embedded concrete columns armed with carbon nanotubes", *Comput. Concrete*, **17**(5), 567–578. https://doi.org/10.12989/CAC.2016.17.5.567.

Kaddari, M., Kaci, A., Bousahla, A.A., Tounsi, A., Bourada, F., Bedia, E.A. and Al-Osta, M.A. (2020), "A study on the structural behaviour of functionally graded porous plates on elastic foundation using a new quasi-3D model: Bending and free vibration analysis", *Comput. Concrete*, **25**(1), 37. https://doi.org/10.12989/cac.2020.25.1.03.

Kim, J., Żur, K.K. and Reddy, J.N. (2019), "Bending, free vibration, and buckling of modified couples stress-based functionally graded porous micro-plates", *Compos. Struct.*, **209**, 879-888. https://doi.org/10.1016/j.compstruct.2018.11.023.

Li, L., Hu, Y. and Ling, L. (2016), "Wave propagation in viscoelastic single-walled carbon nanotubes with surface effect under magnetic field based on nonlocal strain gradient theory", *Physica E.*, **75**, 118-124. https://doi.org/10.1016/j.physe.2015.09.028.

Lim, C.W., Zhang, G. and Reddy, J.N. (2015), "A higher-order nonlocal elasticity and strain gradient theory and its applications in wave propagation", *J. Mech. Phys. Solid.*, **78**, 298-313. https://doi.org/10.1016/j.jmps.2015.02.001.

Lu, L., Guo, X. and Zhao, J. (2019), "A unified size-dependent plate model based on nonlocal strain gradient theory including surface effects", *Appl. Math. Model.*, **68**, 583-602. https://doi.org/10.1016/j.apm.2018.11.023.

Malikan, M. (2020), "On the plastic buckling of curved carbon nanotubes", *Theor. Appl. Mech. Lett.*, **10**(1), 46-56. https://doi.org/10.1016/j.taml.2020.01.004.

Malikan, M. and Eremeyev, V.A. (2020a), "On the dynamics of a visco–piezo–flexoelectric nanobeam", *Symmetry*, **12**(4), 643. https://doi.org/10.3390/sym12040643.

Malikan, M. and Eremeyev, V.A. (2020b), "Post-critical buckling of truncated conical carbon nanotubes considering surface effects embedding in a nonlinear Winkler substrate using the Rayleigh-Ritz method", *Mater. Res. Express.*, **7**(2), 025005. https://doi.org/10.1088/2053-1591/ab691c.

Malikan, M. and Nguyen, V.B. (2018), "Buckling analysis of piezo-magnetoelectric nanoplates in hygrothermal environment based on a novel one variable plate theory combining with higher-order nonlocal strain gradient theory", *Physica E Low Dimens. Syst. Nanostruct.*, **102**, 8-28. https://doi.org/10.1016/j.physe.2018.04.018.

Malikan, M., Dimitri, R. and Tornabene, F. (2019), "Transient response of oscillated carbon nanotubes with an internal and external damping", *Compos. Part B-Eng.*, **158**, 198-205. https://doi.org/10.1016/j.compositesb.2018.09.092.

Malikan, M., Krasheninnikov, M. and Eremeyev, V.A. (2020), "Torsional stability capacity of a nano-composite shell based on a nonlocal strain gradient shell model under a three-dimensional magnetic field", *Int. J. Eng. Sci.*, **148**, 103210. https://doi.org/10.1016/j.ijengsci.2019.103210.

Malikan, M., Nguyen, V.B. and Tornabene, F. (2018a), "Damped forced vibration analysis of single-walled carbon nanotubes resting on viscoelastic foundation in thermal environment using nonlocal strain gradient theory", *Eng. Sci. Tech. Int. J.*, **21**(4), 778-786. https://doi.org/10.1016/j.jestch.2018.06.001.

Malikan, M., Nguyen, V.B. and Tornabene, F. (2018b), "Electromagnetic forced vibrations of composite nanoplates using nonlocal strain gradient theory", *Mater. Res. Express*, **5**(7), 075031. https://doi.org/10.1088/2053-1591/aad144.

Malikan, M., Tornabene, F. and Dimitri, R. (2018c), "Nonlocal three-dimensional theory of elasticity for buckling behavior of functionally graded porous nanoplates using volume integrals", *Mater. Res. Express*, **5**(9), 095006. https://doi.org/10.1088/2053-1591/aad4c3.

Mohammadimehr, M. and Alimirzaei, S. (2016), "Nonlinear static and vibration analysis of Euler-Bernoulli composite beam model reinforced by FG-SWCNT with initial geometrical imperfection using FEM", *Struct. Eng. Mech.*, **59**(3), 431-454. https://doi.org/10.12989/sem.2016.59.3.431.

Mohammadimehr, M., Akhavan Alavi, SM., Okhravi, SV. and Edjtahed, SH. (2018b), "Free vibration analysis of micromagneto-electro-elastic cylindrical sandwich panel considering functionally graded carbon nanotube–reinforced nanocomposite face sheets, various circuit boundary conditions, and temperature-dependent material properties using high-order sandwich panel theory and modified strain gradient theory", *J. Intel. Mater. Syst. Struct.*, **29**(5), 863-882. https://doi.org/10.1177/1045389X17721048.

Mohammadimehr, M., Mohammadi-Najafabadi, M.M., Nasiri, H. and Rousta-Navi, B. (2016a), "Surface stress effects on the free vibration and bending analysis of the nonlocal single-layer graphene sheet embedded in an elastic medium using energy method', *Proc. Inst. Mech. Eng. Part. N*, **230**(3), 148-160. https://doi.org/10.1177%2F1740349914559042.

Mohammadimehr, M., Mohammadimehr, M.A. and Dashti, P. (2016d), "Size-dependent effect on biaxial and shear nonlinear buckling analysis of nonlocal isotropic and orthotropic micro-plate based on surface stress and modified couple stress theories using differential quadrature method", *Appl. Math. Mech.*, **37**(4), 529-554. https://doi.org/10.1007/s10483-016-2045-9.

Mohammadimehr, M., Navi, B.R. and Ghorbanpour Arani, A. (2017b), "Dynamic stability of modified strain gradient theory sinusoidal viscoelastic piezoelectric polymeric functionally graded single-walled carbon nanotubes reinforced nanocomposite plate considering surface stress and agglomeration effects under hydro-thermo-electro-magneto-mechanical loadings", *Mech. Adv. Mater. Struct.*, **24**(16), 1325-1342. https://doi.org/10.1080/15376494.2016.1227507.

Mohammadimehr, M., Rousta-Navi, B. and Ghorbanpour-Arani, A. (2015), "Free vibration of viscoelastic double-bonded polymeric nanocomposite plates reinforced by FG-SWCNTs using MSGT, sinusoidal shear deformation theory and meshless method", *Compos. Struct.*, **131**, 654-671. https://doi.org/10.1016/j.compstruct.2015.05.077.

Mohammadimehr, M., Rousta-Navi, B. and Ghorbanpour-Arani, A. (2016c), "Modified strain gradient Reddy rectangular plate

model for biaxial buckling and bending analysis of double-coupled piezoelectric polymeric nanocomposite reinforced by FG-SWNT", *Compos. Part B. Eng.*, **87**, 132-148. https://doi.org/10.1016/j.compositesb.2015.10.007.

Mohammadimehr, M., Salemi, M. and Rousta-Navi, B. (2016b), "Bending, buckling, and free vibration analysis of MSGT microcomposite Reddy plate reinforced by FG-SWCNTs with temperature-dependent material properties under hydro-thermo-mechanical loadings using DQM", *Compos. Struct.*, **138**, 361-380. https://doi.org/10.1016/j.compstruct.2015.11.055.

Mohammadimehr, M., Shabani-Nejad, E. and Mehrabi, M. (2018a), "Buckling and vibration analyses of MGSGT double-bonded micro composite sandwich SSDT plates reinforced by CNTs and BNNTs with isotropic foam & flexible transversely orthotropic cores", *Struct. Eng. Mech.*, **65**(4), 491-504. https://doi.org/10.12989/sem.2018.65.4.491.

Mohammadimehr, M., Shahedi, S. and Rousta Navi, B. (2017a), "Nonlinear vibration analysis of FG-CNTRC sandwich Timoshenko beam based on modified couple stress theory subjected to longitudinal magnetic field using generalized differential quadrature method", *Proc. Inst. Mech. Eng., Part C: J. Mech. Eng. Sci.*, **231**(20), 3866-3885. https://doi.org/10.1177/0954406216653622

Moradi-Dastjerdi, R., Malek-Mohammadi, H. and Momeni-Khabisi, H. (2017), "Free vibration analysis of nanocomposite sandwich plates reinforced with CNT aggregates", *Z. Angew. Math. Mech.*, **97**(11), 1418-1435. https://doi.org/10.1002/zamm.201600209.

Mousavi, M., Mohammadimehr, M. and Rostami, R. (2019), "Analytical solution for buckling analysis of micro sandwich hollow circular plate", *Comput. Concrete*, **24**(3), 185-192. https://doi.org/10.12989/cac.2019.24.3.185.

Rajabi, J. and Mohammadimehr, M. (2019), "Bending analysis of a micro sandwich skew plate using extended Kantorovich method based on Eshelby-Mori-Tanaka approach", *Comput. Concrete*, **23**(5), 361-376. https://doi.org/10.12989/cac.2019.23.5.361.

Rezaei, A.S. and Saidi, A.R. (2015), "Exact solution for free vibration of thick rectangular plates made of porous materials", *Compos. Struct.*, **134**, 1051-1060. https://doi.org/10.1016/j.compstruct.2015.08.125.

Rezaei, A.S., Saidi, A.R., Abrishamdari, M. and Mohammadi, M.P. (2017), "Natural frequencies of functionally graded plates with porosities via a simple four variable plate theory: an analytical approach", *Thin Wall. Struct.*, **120**, 366-377. https://doi.org/10.1016/j.tws.2017.08.003.

She, G.L., Yan, K.M., Zhang, Y.L., Liu, H.B. and Ren, Y.R. (2018a), "Wave propagation of functionally graded porous nanobeams based on non-local strain gradient theory", *Eur. Phys. J. Plus.*, **133**(9), 368. https://doi.org/10.1140/epjp/i2018-12196-5.

She, G.L., Yuan, F.G., Ren, Y.R., Liu, H.B. and Xiao, W.S. (2018b), "Nonlinear bending and vibration analysis of functionally graded porous tubes via a nonlocal strain gradient theory", *Compos. Struct.*, **203**, 614-623. https://doi.org/10.1016/j.compstruct.2018.07.063.

Tanzadeh, H. and Amoushahi, H. (2019), "Buckling and free vibration analysis of piezoelectric laminated composite plates using various plate deformation theories', *Eur. J. Mech. A. Solid.*, **74**, 242-256. https://doi.org/10.1016/j.euromechsol.2018.11.013.

Thai, H.T. and Choi, D.H. (2013), "Size-dependent functionally graded Kirchhoff and Mindlin plate models based on a modified couple stress theory", *Compos. Struct.*, **95**, 142-153. https://doi.org/10.1016/j.compstruct.2012.08.023.

Thai, H.T. and Kim, S.E. (2013), "A size-dependent functionally graded Reddy plate model based on a modified couple stress theory", *Compos. Part. B. Eng.*, **45**(1), 1636-1645. https://doi.org/10.1016/j.compositesb.2012.09.065.

Van Do, T., Nguyen, D.K., Duc, N.D., Doan, D.H. and Bui, T.Q. (2017), "Analysis of bi-directional functionally graded plates by FEM and a new third-order shear deformation plate theory", *Thin Wall. Struct.*, **119**, 687-699. https://doi.org/10.1016/j.tws.2017.07.022.

Yang, J., Chen, D. and Kitipornchai, S. (2018), "Buckling and free vibration analyses of functionally graded graphene reinforced porous nanocomposite plates based on Chebyshev-Ritz method", *Compos. Struct.*, **193**, 281-294. https://doi.org/10.1016/j.compstruct.2018.03.090.

Zenkour, A.M. and Alghanmi, R.A. (2019), "Stress analysis of a functionally graded plate integrated with piezoelectric faces via a four-unknown shear deformation theory", *Resul. Phys.*, **12**, 268-277. https://doi.org/10.1016/j.rinp.2018.11.045.

Zhang, D.P., Lei, Y. and Shen, Z.B. (2018), "Semi-analytical solution for vibration of nonlocal piezoelectric Kirchhoff plates resting on viscoelastic foundation", *J. Appl. Comput. Mech.*, **4**(3), 202-215. https://dx.doi.org/10.22055/jacm.2017.23096.1149.

CC

Appendix A

$$N_x = \frac{1}{1-\upsilon^2}\times$$

$$\left(\begin{array}{l} A_x^0\frac{\partial u_0}{\partial x}-A_x^1\frac{\partial^2 w}{\partial x^2}+\upsilon\left(A_x^0\frac{\partial v_0}{\partial y}-A_x^1\frac{\partial^2 w}{\partial y^2}\right) \\ -\ell^2\left(\begin{array}{l} A_x^0\frac{\partial^3 u_0}{\partial x^3}-A_x^1\frac{\partial^4 w}{\partial x^4}+\upsilon\left(A_x^0\frac{\partial^3 v_0}{\partial x^2\partial y}-A_x^1\frac{\partial^4 w}{\partial x^2\partial y^2}\right) \\ +A_x^0\frac{\partial^3 u_0}{\partial x\,\partial y^2}-A_x^1\frac{\partial^4 w}{\partial x^2\partial y^2}+\upsilon\left(A_x^0\frac{\partial^3 v_0}{\partial y^3}-A_x^1\frac{\partial^4 w}{\partial y^4}\right) \end{array}\right) \\ +\tau_d\left(A_x^0\frac{\partial^2 u_0}{\partial x\,\partial t}-A_x^1\frac{\partial^3 w}{\partial x^2\partial t}+\upsilon\left(A_x^0\frac{\partial^2 v_0}{\partial y\,\partial t}-A_x^1\frac{\partial^3 w}{\partial y^2\partial t}\right)\right) \\ -\tau_d\ell^2\left(\begin{array}{l} A_x^0\frac{\partial^4 u_0}{\partial x^3\partial t}-A_x^1\frac{\partial^5 w}{\partial x^4\partial t}+\upsilon\left(A_x^0\frac{\partial^4 v_0}{\partial x^2\partial y\,\partial t}-A_x^1\frac{\partial^5 w}{\partial x^2\partial y^2\partial t}\right) \\ +A_x^0\frac{\partial^4 u_0}{\partial x\,\partial y^2\partial t}-A_x^1\frac{\partial^5 w}{\partial x^2\partial y^2\partial t}+\upsilon\left(A_x^0\frac{\partial^4 v_0}{\partial y^3\partial t}-A_x^1\frac{\partial^5 w}{\partial y^4\partial t}\right) \end{array}\right) \end{array}\right)$$

$$+\frac{(e_0a)^2}{1-\upsilon^2}\times$$

$$\left(\begin{array}{l} A_x^0\frac{\partial^3 u_0}{\partial x^3}-A_x^1\frac{\partial^4 w}{\partial x^4}+\upsilon\left(A_x^0\frac{\partial^3 v_0}{\partial x^2\partial y}-A_x^1\frac{\partial^4 w}{\partial x^2\partial y^2}\right) \\ -\ell^2\left(\begin{array}{l} A_x^0\frac{\partial^5 u_0}{\partial x^5}-A_x^1\frac{\partial^6 w}{\partial x^6}+\upsilon\left(A_x^0\frac{\partial^5 v_0}{\partial x^4\partial y}-A_x^1\frac{\partial^6 w}{\partial x^4\partial y^2}\right) \\ +A_x^0\frac{\partial^5 u_0}{\partial x^3\partial y^2}-A_x^1\frac{\partial^6 w}{\partial x^4\partial y^2}+\upsilon\left(A_x^0\frac{\partial^5 v_0}{\partial x^2\partial y^3}-A_x^1\frac{\partial^6 w}{\partial x^2\partial y^4}\right) \end{array}\right) \\ +\tau_d\left(A_x^0\frac{\partial^4 u_0}{\partial x^3\partial t}-A_x^1\frac{\partial^5 w}{\partial x^4\partial t}+\upsilon\left(A_x^0\frac{\partial^4 v_0}{\partial x^2\partial y\,\partial t}-A_x^1\frac{\partial^5 w}{\partial x^2\partial y^2\partial t}\right)\right) \\ -\tau_d\ell^2\left(\begin{array}{l} A_x^0\frac{\partial^6 u_0}{\partial x^5\partial t}-A_x^1\frac{\partial^7 w}{\partial x^6\partial t}+\upsilon\left(A_x^0\frac{\partial^6 v_0}{\partial x^4\partial y\,\partial t}-A_x^1\frac{\partial^7 w}{\partial x^4\partial y^2\partial t}\right) \\ +A_x^0\frac{\partial^6 u_0}{\partial x^3\partial y^2\partial t}-A_x^1\frac{\partial^7 w}{\partial x^4\partial y^2\partial t}+\upsilon\left(A_x^0\frac{\partial^6 v_0}{\partial x^2\partial y^3\partial t}-A_x^1\frac{\partial^7 w}{\partial x^2\partial y^4\partial t}\right) \end{array}\right) \end{array}\right) \quad \text{(A.1)}$$

$$+\frac{(e_0a)^2}{1-\upsilon^2}\times$$

$$\left(\begin{array}{l} A_x^0\frac{\partial^3 u_0}{\partial x\,\partial y^2}-A_x^1\frac{\partial^4 w}{\partial x^2\partial y^2}+\upsilon\left(A_x^0\frac{\partial^3 v_0}{\partial y^3}-A_x^1\frac{\partial^4 w}{\partial y^4}\right) \\ -\ell^2\left(\begin{array}{l} A_x^0\frac{\partial^5 u_0}{\partial x^3\partial y^2}-A_x^1\frac{\partial^6 w}{\partial x^4\partial y^2}+\upsilon\left(A_x^0\frac{\partial^5 v_0}{\partial x^2\partial y^3}-A_x^1\frac{\partial^6 w}{\partial x^2\partial y^4}\right) \\ +A_x^0\frac{\partial^5 u_0}{\partial x\,\partial y^4}-A_x^1\frac{\partial^6 w}{\partial x^2\partial y^4}+\upsilon\left(A_x^0\frac{\partial^5 v_0}{\partial y^5}-A_x^1\frac{\partial^6 w}{\partial y^6}\right) \end{array}\right) \\ +\tau_d\left(A_x^0\frac{\partial^4 u_0}{\partial x\,\partial y^2\partial t}-A_x^1\frac{\partial^5 w}{\partial x^2\partial y^2\partial t}+\upsilon\left(A_x^0\frac{\partial^4 v_0}{\partial y^3\partial t}-A_x^1\frac{\partial^5 w}{\partial y^4\partial t}\right)\right) \\ -\tau_d\ell^2\left(\begin{array}{l} A_x^0\frac{\partial^6 u_0}{\partial x^3\partial y^2\partial t}-A_x^1\frac{\partial^7 w}{\partial x^4\partial y^2\partial t}+\upsilon\left(A_x^0\frac{\partial^6 v_0}{\partial x^2\partial y^3\partial t}-A_x^1\frac{\partial^7 w}{\partial x^2\partial y^4\partial t}\right) \\ +A_x^0\frac{\partial^6 u_0}{\partial x\,\partial y^4\partial t}-A_x^1\frac{\partial^7 w}{\partial x^2\partial y^4\partial t}+\upsilon\left(A_x^0\frac{\partial^6 v_0}{\partial y^5\partial t}-A_x^1\frac{\partial^7 w}{\partial y^6\partial t}\right) \end{array}\right) \end{array}\right)$$

$$-e_{31}\left(-C^0\beta'\phi_E-B^0\frac{2V_E}{h}\right)+\frac{(e_0a)^2}{1-\upsilon^2}\left(-e_{31}\left(-C^0\beta'\frac{\partial^2\phi_E}{\partial x^2}\right)-e_{31}\left(-C^0\beta'\frac{\partial^2\phi_E}{\partial y^2}\right)\right)$$

$$N_y = \frac{1}{1-\upsilon^2}\times$$

$$\left(\begin{array}{l} A_y^0\frac{\partial v_0}{\partial y}-A_y^1\frac{\partial^2 w}{\partial y^2}+\upsilon\left(A_x^0\frac{\partial u_0}{\partial x}-A_x^1\frac{\partial^2 w}{\partial x^2}\right) \\ -\ell^2\left(\begin{array}{l} A_y^0\frac{\partial^3 v_0}{\partial x^2\partial y}-A_y^1\frac{\partial^4 w}{\partial x^2\partial y^2}+\upsilon\left(A_x^0\frac{\partial^3 u_0}{\partial x^3}-A_x^1\frac{\partial^4 w}{\partial x^4}\right) \\ +A_y^0\frac{\partial^3 v_0}{\partial y^3}-A_y^1\frac{\partial^4 w}{\partial y^4}+\upsilon\left(A_x^0\frac{\partial^3 u_0}{\partial x\,\partial y^2}-A_x^1\frac{\partial^4 w}{\partial x^2\partial y^2}\right) \end{array}\right) \\ +\tau_d\left(A_y^0\frac{\partial^2 v_0}{\partial y\,\partial t}-A_y^1\frac{\partial^3 w}{\partial y^2\partial t}+\upsilon\left(A_x^0\frac{\partial^2 u_0}{\partial x\,\partial t}-A_x^1\frac{\partial^3 w}{\partial x^2\partial t}\right)\right) \\ -\tau_d\ell^2\left(\begin{array}{l} A_y^0\frac{\partial^4 v_0}{\partial x^2\partial y\,\partial t}-A_y^1\frac{\partial^5 w}{\partial x^2\partial y^2\partial t}+\upsilon\left(A_x^0\frac{\partial^4 u_0}{\partial x^3\partial t}-A_x^1\frac{\partial^5 w}{\partial x^4\partial t}\right) \\ +A_y^0\frac{\partial^4 v_0}{\partial y^3\partial t}-A_y^1\frac{\partial^5 w}{\partial y^4\partial t}+\upsilon\left(A_x^0\frac{\partial^4 u_0}{\partial x\,\partial y^2\partial t}-A_x^1\frac{\partial^5 w}{\partial x^2\partial y^2\partial t}\right) \end{array}\right) \end{array}\right) \quad \text{(A.2)}$$

$$+\frac{(e_0a)^2}{1-\upsilon^2}\times$$

$$\left(\begin{array}{l} A_y^0\frac{\partial^3 v_0}{\partial x^2\partial y}-A_y^1\frac{\partial^4 w}{\partial x^2\partial y^2}+\upsilon\left(A_x^0\frac{\partial^3 u_0}{\partial x^3}-A_x^1\frac{\partial^4 w}{\partial x^4}\right) \\ -\ell^2\left(\begin{array}{l} A_y^0\frac{\partial^5 v_0}{\partial x^4\partial y}-A_y^1\frac{\partial^6 w}{\partial x^4\partial y^2}+\upsilon\left(A_x^0\frac{\partial^5 u_0}{\partial x^5}-A_x^1\frac{\partial^6 w}{\partial x^6}\right) \\ +A_y^0\frac{\partial^5 v_0}{\partial x^2\partial y^3}-A_y^1\frac{\partial^6 w}{\partial x^2\partial y^4}+\upsilon\left(A_x^0\frac{\partial^5 u_0}{\partial x^3\partial y^2}-A_x^1\frac{\partial^6 w}{\partial x^4\partial y^2}\right) \end{array}\right) \\ +\tau_d\left(A_y^0\frac{\partial^4 v_0}{\partial x^2\partial y\,\partial t}-A_y^1\frac{\partial^5 w}{\partial x^2\partial y^2\partial t}+\upsilon\left(A_x^0\frac{\partial^4 u_0}{\partial x^3\partial t}-A_x^1\frac{\partial^5 w}{\partial x^4\partial t}\right)\right) \\ -\tau_d\ell^2\left(\begin{array}{l} A_y^0\frac{\partial^6 v_0}{\partial x^4\partial y\,\partial t}-A_y^1\frac{\partial^7 w}{\partial x^4\partial y^2\partial t}+\upsilon\left(A_x^0\frac{\partial^6 u_0}{\partial x^5\partial t}-A_x^1\frac{\partial^7 w}{\partial x^6\partial t}\right) \\ +A_y^0\frac{\partial^6 v_0}{\partial x^2\partial y^3\partial t}-A_y^1\frac{\partial^7 w}{\partial x^2\partial y^4\partial t}+\upsilon\left(A_x^0\frac{\partial^6 u_0}{\partial x^3\partial y^2\partial t}-A_x^1\frac{\partial^7 w}{\partial x^4\partial y^2\partial t}\right) \end{array}\right) \end{array}\right) \quad \text{(A.2)}$$

$$+\frac{(e_0a)^2}{1-\upsilon^2}\times$$

$$\left(\begin{array}{l} A_y^0\frac{\partial^3 v_0}{\partial y^3}-A_y^1\frac{\partial^4 w}{\partial y^4}+\upsilon\left(A_x^0\frac{\partial^3 u_0}{\partial x\,\partial y^2}-A_x^1\frac{\partial^4 w}{\partial x^2\partial y^2}\right) \\ -\ell^2\left(\begin{array}{l} A_y^0\frac{\partial^5 v_0}{\partial x^2\partial y^3}-A_y^1\frac{\partial^6 w}{\partial x^2\partial y^4}+\upsilon\left(A_x^0\frac{\partial^5 u_0}{\partial x^3\partial y^2}-A_x^1\frac{\partial^6 w}{\partial x^4\partial y^2}\right) \\ +A_y^0\frac{\partial^5 v_0}{\partial y^5}-A_y^1\frac{\partial^6 w}{\partial y^6}+\upsilon\left(A_x^0\frac{\partial^5 u_0}{\partial x\,\partial y^4}-A_x^1\frac{\partial^6 w}{\partial x^2\partial y^4}\right) \end{array}\right) \\ +\tau_d\left(A_y^0\frac{\partial^4 v_0}{\partial y^3\partial t}-A_y^1\frac{\partial^5 w}{\partial y^4\partial t}+\upsilon\left(A_x^0\frac{\partial^4 u_0}{\partial x\,\partial y^2\partial t}-A_x^1\frac{\partial^5 w}{\partial x^2\partial y^2\partial t}\right)\right) \\ -\tau_d\ell^2\left(\begin{array}{l} A_y^0\frac{\partial^6 v_0}{\partial x^2\partial y^3\partial t}-A_y^1\frac{\partial^7 w}{\partial x^2\partial y^4\partial t}+\upsilon\left(A_x^0\frac{\partial^6 u_0}{\partial x^3\partial y^2\partial t}-A_x^1\frac{\partial^7 w}{\partial x^4\partial y^2\partial t}\right) \\ +A_y^0\frac{\partial^6 v_0}{\partial y^5\partial t}-A_y^1\frac{\partial^7 w}{\partial y^6\partial t}+\upsilon\left(A_x^0\frac{\partial^6 u_0}{\partial x\,\partial y^4\partial t}-A_x^1\frac{\partial^7 w}{\partial x^2\partial y^4\partial t}\right) \end{array}\right) \end{array}\right)$$

$$-e_{32}\left(-C^0\beta'\phi_E-B^0\frac{2V_E}{h}\right)+\frac{(e_0a)^2}{1-\upsilon^2}\left(-e_{32}\left(-C^0\beta'\frac{\partial^2\phi_E}{\partial x^2}\right)-e_{32}\left(-C^0\beta'\frac{\partial^2\phi_E}{\partial y^2}\right)\right)$$

$$
\begin{aligned}
N_{xy} = & \\
& \left(\begin{array}{l}
A_{xy}^{0}\dfrac{\partial u_0}{\partial y}+A_{xy}^{0}\dfrac{\partial v_0}{\partial x}-2A_{xy}^{1}\dfrac{\partial^2 w}{\partial x\,\partial y} \\
-\ell^2\left(\begin{array}{l} A_{xy}^{0}\dfrac{\partial^3 u_0}{\partial x^2\partial y}+A_{xy}^{0}\dfrac{\partial^3 v_0}{\partial x^3}-2A_{xy}^{1}\dfrac{\partial^4 w}{\partial x^3\partial y} \\ +A_{xy}^{0}\dfrac{\partial^3 u_0}{\partial y^3}+A_{xy}^{0}\dfrac{\partial^3 v_0}{\partial x\,\partial y^2}-2A_{xy}^{1}\dfrac{\partial^4 w}{\partial x\,\partial y^3} \end{array} \right) \\
+\tau_d\left(A_{xy}^{0}\dfrac{\partial^2 u_0}{\partial y\,\partial t}+A_{xy}^{0}\dfrac{\partial^2 v_0}{\partial x\,\partial t}-2A_{xy}^{1}\dfrac{\partial^3 w}{\partial x\,\partial y\,\partial t} \right) \\
-\tau_d\ell^2\left(\begin{array}{l} A_{xy}^{0}\dfrac{\partial^4 u_0}{\partial x^2\partial y\,\partial t}+A_{xy}^{0}\dfrac{\partial^4 v_0}{\partial x^3\partial t}-2A_{xy}^{1}\dfrac{\partial^5 w}{\partial x^3\partial y\,\partial t} \\ +A_{xy}^{0}\dfrac{\partial^4 u_0}{\partial y^3\partial t}+A_{xy}^{0}\dfrac{\partial^4 v_0}{\partial x\,\partial y^2\partial t}-2A_{xy}^{1}\dfrac{\partial^5 w}{\partial x\,\partial y^3\partial t} \end{array} \right)
\end{array} \right) \\
& +(e_0a)^2 \left(\begin{array}{l}
A_{xy}^{0}\dfrac{\partial^3 u_0}{\partial x^2\partial y}+A_{xy}^{0}\dfrac{\partial^3 v_0}{\partial x^3}-2A_{xy}^{1}\dfrac{\partial^4 w}{\partial x^3\partial y} \\
-\ell^2\left(\begin{array}{l} A_{xy}^{0}\dfrac{\partial^5 u_0}{\partial x^4\partial y}+A_{xy}^{0}\dfrac{\partial^5 v_0}{\partial x^5}-2A_{xy}^{1}\dfrac{\partial^6 w}{\partial x^5\partial y} \\ +A_{xy}^{0}\dfrac{\partial^5 u_0}{\partial x^2\partial y^3}+A_{xy}^{0}\dfrac{\partial^5 v_0}{\partial x^3\partial y^2}-2A_{xy}^{1}\dfrac{\partial^6 w}{\partial x^3\partial y^3} \end{array} \right) \\
+\tau_d\left(A_{xy}^{0}\dfrac{\partial^4 u_0}{\partial x^2\partial y\,\partial t}+A_{xy}^{0}\dfrac{\partial^4 v_0}{\partial x^3\partial t}-2A_{xy}^{1}\dfrac{\partial^5 w}{\partial x^3\partial y\,\partial t} \right) \\
-\tau_d\ell^2\left(\begin{array}{l} A_{xy}^{0}\dfrac{\partial^6 u_0}{\partial x^4\partial y\,\partial t}+A_{xy}^{0}\dfrac{\partial^6 v_0}{\partial x^5\partial t}-2A_{xy}^{1}\dfrac{\partial^7 w}{\partial x^5\partial y\,\partial t} \\ +A_{xy}^{0}\dfrac{\partial^6 u_0}{\partial x^2\partial y^3\partial t}+A_{xy}^{0}\dfrac{\partial^6 v_0}{\partial x^3\partial y^2\partial t}-2A_{xy}^{1}\dfrac{\partial^7 w}{\partial x^3\partial y^3\partial t} \end{array} \right)
\end{array} \right) \\
& +(e_0a)^2 \left(\begin{array}{l}
A_{xy}^{0}\dfrac{\partial^3 u_0}{\partial y^3}+A_{xy}^{0}\dfrac{\partial^3 v_0}{\partial x\,\partial y^2}-2A_{xy}^{1}\dfrac{\partial^4 w}{\partial x\,\partial y^3} \\
-\ell^2\left(\begin{array}{l} A_{xy}^{0}\dfrac{\partial^5 u_0}{\partial x^2\partial y^3}+A_{xy}^{0}\dfrac{\partial^5 v_0}{\partial x^3\partial y^2}-2A_{xy}^{1}\dfrac{\partial^6 w}{\partial x^3\partial y^3} \\ +A_{xy}^{0}\dfrac{\partial^5 u_0}{\partial y^5}+A_{xy}^{0}\dfrac{\partial^5 v_0}{\partial x\,\partial y^4}-2A_{xy}^{1}\dfrac{\partial^6 w}{\partial x\,\partial y^5} \end{array} \right) \\
+\tau_d\left(A_{xy}^{0}\dfrac{\partial^4 u_0}{\partial y^3\partial t}+A_{xy}^{0}\dfrac{\partial^4 v_0}{\partial x\,\partial y^2\partial t}-2A_{xy}^{1}\dfrac{\partial^5 w}{\partial x\,\partial y^3\partial t} \right) \\
-\tau_d\ell^2\left(\begin{array}{l} A_{xy}^{0}\dfrac{\partial^6 u_0}{\partial x^2\partial y^3\partial t}+A_{xy}^{0}\dfrac{\partial^6 v_0}{\partial x^3\partial y^2\partial t}-2A_{xy}^{1}\dfrac{\partial^7 w}{\partial x^3\partial y^3\partial t} \\ +A_{xy}^{0}\dfrac{\partial^6 u_0}{\partial y^5\partial t}+A_{xy}^{0}\dfrac{\partial^6 v_0}{\partial x\,\partial y^4\partial t}-2A_{xy}^{1}\dfrac{\partial^7 w}{\partial x\,\partial y^5\partial t} \end{array} \right)
\end{array} \right)
\end{aligned}
\tag{A.3}
$$

$$
\begin{aligned}
M_x = & \frac{1}{1-\upsilon^2}\times \\
& \left(\begin{array}{l}
A_x^{1}\dfrac{\partial u_0}{\partial x}-A_x^{2}\dfrac{\partial^2 w}{\partial x^2}+\upsilon\left(A_x^{1}\dfrac{\partial v_0}{\partial y}-A_x^{2}\dfrac{\partial^2 w}{\partial y^2} \right) \\
-\ell^2\left(\begin{array}{l} A_x^{1}\dfrac{\partial^3 u_0}{\partial x^3}-A_x^{2}\dfrac{\partial^4 w}{\partial x^4}+\upsilon\left(A_x^{1}\dfrac{\partial^3 v_0}{\partial x^2\partial y}-A_x^{2}\dfrac{\partial^4 w}{\partial x^2\partial y^2} \right) \\ +A_x^{1}\dfrac{\partial^3 u_0}{\partial x\,\partial y^2}-A_x^{2}\dfrac{\partial^4 w}{\partial x^2\partial y^2}+\upsilon\left(A_x^{1}\dfrac{\partial^3 v_0}{\partial y^3}-A_x^{2}\dfrac{\partial^4 w}{\partial y^4} \right) \end{array} \right) \\
+\tau_d\left(A_x^{1}\dfrac{\partial^2 u_0}{\partial x\,\partial t}-A_x^{2}\dfrac{\partial^3 w}{\partial x^2\partial t}+\upsilon\left(A_x^{1}\dfrac{\partial^2 v_0}{\partial y\,\partial t}-A_x^{2}\dfrac{\partial^3 w}{\partial y^2\partial t} \right) \right) \\
-\tau_d\ell^2\left(\begin{array}{l} A_x^{1}\dfrac{\partial^4 u_0}{\partial x^3\partial t}-A_x^{2}\dfrac{\partial^5 w}{\partial x^4\partial t}+\upsilon\left(A_x^{1}\dfrac{\partial^4 v_0}{\partial x^2\partial y\,\partial t}-A_x^{2}\dfrac{\partial^5 w}{\partial x^2\partial y^2\partial t} \right) \\ +A_x^{1}\dfrac{\partial^4 u_0}{\partial x\,\partial y^2\partial t}-A_x^{2}\dfrac{\partial^5 w}{\partial x^2\partial y^2\partial t}+\upsilon\left(A_x^{1}\dfrac{\partial^4 v_0}{\partial y^3\partial t}-A_x^{2}\dfrac{\partial^5 w}{\partial y^4\partial t} \right) \end{array} \right)
\end{array} \right) \\
& +\frac{(e_0a)^2}{1-\upsilon^2}\times \\
& \left(\begin{array}{l}
A_x^{1}\dfrac{\partial^3 u_0}{\partial x^3}-A_x^{2}\dfrac{\partial^4 w}{\partial x^4}+\upsilon\left(A_x^{1}\dfrac{\partial^3 v_0}{\partial x^2\partial y}-A_x^{2}\dfrac{\partial^4 w}{\partial x^2\partial y^2} \right) \\
-\ell^2\left(\begin{array}{l} A_x^{1}\dfrac{\partial^5 u_0}{\partial x^5}-A_x^{2}\dfrac{\partial^6 w}{\partial x^6}+\upsilon\left(A_x^{1}\dfrac{\partial^5 v_0}{\partial x^4\partial y}-A_x^{2}\dfrac{\partial^6 w}{\partial x^4\partial y^2} \right) \\ +A_x^{1}\dfrac{\partial^5 u_0}{\partial x^3\partial y^2}-A_x^{2}\dfrac{\partial^6 w}{\partial x^4\partial y^2}+\upsilon\left(A_x^{1}\dfrac{\partial^5 v_0}{\partial x^2\partial y^3}-A_x^{2}\dfrac{\partial^6 w}{\partial x^2\partial y^4} \right) \end{array} \right) \\
+\tau_d\left(A_x^{1}\dfrac{\partial^4 u_0}{\partial x^3\partial t}-A_x^{2}\dfrac{\partial^5 w}{\partial x^4\partial t}+\upsilon\left(A_x^{1}\dfrac{\partial^4 v_0}{\partial x^2\partial y\,\partial t}-A_x^{2}\dfrac{\partial^5 w}{\partial x^2\partial y^2\partial t} \right) \right) \\
-\tau_d\ell^2\left(\begin{array}{l} A_x^{1}\dfrac{\partial^6 u_0}{\partial x^5\partial t}-A_x^{2}\dfrac{\partial^7 w}{\partial x^6\partial t}+\upsilon\left(A_x^{1}\dfrac{\partial^6 v_0}{\partial x^4\partial y\,\partial t}-A_x^{2}\dfrac{\partial^7 w}{\partial x^4\partial y^2\partial t} \right) \\ +A_x^{1}\dfrac{\partial^6 u_0}{\partial x^3\partial y^2\partial t}-A_x^{2}\dfrac{\partial^7 w}{\partial x^4\partial y^2\partial t}+\upsilon\left(A_x^{1}\dfrac{\partial^6 v_0}{\partial x^2\partial y^3\partial t}-A_x^{2}\dfrac{\partial^7 w}{\partial x^2\partial y^4\partial t} \right) \end{array} \right)
\end{array} \right) \\
& +\frac{(e_0a)^2}{1-\upsilon^2}\times \\
& \left(\begin{array}{l}
A_x^{1}\dfrac{\partial^3 u_0}{\partial x\,\partial y^2}-A_x^{2}\dfrac{\partial^4 w}{\partial x^2\partial y^2}+\upsilon\left(A_x^{1}\dfrac{\partial^3 v_0}{\partial y^3}-A_x^{2}\dfrac{\partial^4 w}{\partial y^4} \right) \\
-\ell^2\left(\begin{array}{l} A_x^{1}\dfrac{\partial^5 u_0}{\partial x^3\partial y^2}-A_x^{2}\dfrac{\partial^6 w}{\partial x^4\partial y^2}+\upsilon\left(A_x^{1}\dfrac{\partial^5 v_0}{\partial x^2\partial y^3}-A_x^{2}\dfrac{\partial^6 w}{\partial x^2\partial y^4} \right) \\ +A_x^{1}\dfrac{\partial^5 u_0}{\partial x\,\partial y^4}-A_x^{2}\dfrac{\partial^6 w}{\partial x^2\partial y^4}+\upsilon\left(A_x^{1}\dfrac{\partial^5 v_0}{\partial y^5}-A_x^{2}\dfrac{\partial^6 w}{\partial y^6} \right) \end{array} \right) \\
+\tau_d\left(A_x^{1}\dfrac{\partial^4 u_0}{\partial x\,\partial y^2\partial t}-A_x^{2}\dfrac{\partial^5 w}{\partial x^2\partial y^2\partial t}+\upsilon\left(A_x^{1}\dfrac{\partial^4 v_0}{\partial y^3\partial t}-A_x^{2}\dfrac{\partial^5 w}{\partial y^4\partial t} \right) \right) \\
-\tau_d\ell^2\left(\begin{array}{l} A_x^{1}\dfrac{\partial^6 u_0}{\partial x^3\partial y^2\partial t}-A_x^{2}\dfrac{\partial^7 w}{\partial x^4\partial y^2\partial t}+\upsilon\left(A_x^{1}\dfrac{\partial^6 v_0}{\partial x^2\partial y^3\partial t}-A_x^{2}\dfrac{\partial^7 w}{\partial x^2\partial y^4\partial t} \right) \\ +A_x^{1}\dfrac{\partial^6 u_0}{\partial x\,\partial y^4\partial t}-A_x^{2}\dfrac{\partial^7 w}{\partial x^2\partial y^4\partial t}+\upsilon\left(A_x^{1}\dfrac{\partial^6 v_0}{\partial y^5\partial t}-A_x^{2}\dfrac{\partial^7 w}{\partial y^6\partial t} \right) \end{array} \right)
\end{array} \right) \\
& -e_{31}\left(-C^1\beta'\phi_E-B^1\frac{2V_E}{h} \right)+\frac{(e_0a)^2}{1-\upsilon^2}\left(-e_{31}\left(-C^1\beta'\frac{\partial^2\phi_E}{\partial x^2} \right)-e_{31}\left(-C^1\beta'\frac{\partial^2\phi_E}{\partial y^2} \right) \right)
\end{aligned}
\tag{A.4}
$$

$$M_y = \frac{1}{1-\upsilon^2}\times$$
$$\left(\begin{array}{l} A_y^1\frac{\partial v_0}{\partial y}-A_y^2\frac{\partial^2 w}{\partial y^2}+\upsilon\left(A_x^1\frac{\partial u_0}{\partial x}-A_x^2\frac{\partial^2 w}{\partial x^2}\right) \\ -\ell^2\left(\begin{array}{l} A_y^1\frac{\partial^3 v_0}{\partial x^2\partial y}-A_y^2\frac{\partial^4 w}{\partial x^2\partial y^2}+\upsilon\left(A_x^1\frac{\partial^3 u_0}{\partial x^3}-A_x^2\frac{\partial^4 w}{\partial x^4}\right) \\ +A_y^1\frac{\partial^3 v_0}{\partial y^3}-A_y^2\frac{\partial^4 w}{\partial y^4}+\upsilon\left(A_x^1\frac{\partial^3 u_0}{\partial x\partial y^2}-A_x^2\frac{\partial^4 w}{\partial x^2\partial y^2}\right) \end{array}\right) \\ +\tau_d\left(A_y^1\frac{\partial^2 v_0}{\partial y\,\partial t}-A_y^2\frac{\partial^3 w}{\partial y^2\partial t}+\upsilon\left(A_x^1\frac{\partial^2 u_0}{\partial x\partial t}-A_x^2\frac{\partial^3 w}{\partial x^2\partial t}\right)\right) \\ -\tau_d\ell^2\left(\begin{array}{l} A_y^1\frac{\partial^4 v_0}{\partial x^2\partial y\,\partial t}-A_y^2\frac{\partial^5 w}{\partial x^2\partial y^2\partial t}+\upsilon\left(A_x^1\frac{\partial^4 u_0}{\partial x^3\partial t}-A_x^2\frac{\partial^5 w}{\partial x^4\partial t}\right) \\ +A_y^1\frac{\partial^4 v_0}{\partial y^3\partial t}-A_y^2\frac{\partial^5 w}{\partial y^4\partial t}+\upsilon\left(A_x^1\frac{\partial^4 u_0}{\partial x\partial y^2\partial t}-A_x^2\frac{\partial^5 w}{\partial x^2\partial y^2\partial t}\right) \end{array}\right) \end{array}\right) \quad \text{(A.5)}$$
$$+\frac{(e_0a)^2}{1-\upsilon^2}\times$$
$$\left(\begin{array}{l} A_y^1\frac{\partial^3 v_0}{\partial x^2\partial y}-A_y^2\frac{\partial^4 w}{\partial x^2\partial y^2}+\upsilon\left(A_x^1\frac{\partial^3 u_0}{\partial x^3}-A_x^2\frac{\partial^4 w}{\partial x^4}\right) \\ -\ell^2\left(\begin{array}{l} A_y^1\frac{\partial^5 v_0}{\partial x^4\partial y}-A_y^2\frac{\partial^6 w}{\partial x^4\partial y^2}+\upsilon\left(A_x^1\frac{\partial^5 u_0}{\partial x^5}-A_x^2\frac{\partial^6 w}{\partial x^6}\right) \\ +A_y^1\frac{\partial^5 v_0}{\partial x^2\partial y^3}-A_y^2\frac{\partial^6 w}{\partial x^2\partial y^4}+\upsilon\left(A_x^1\frac{\partial^5 u_0}{\partial x^3\partial y^2}-A_x^2\frac{\partial^6 w}{\partial x^4\partial y^2}\right) \end{array}\right) \\ +\tau_d\left(A_y^1\frac{\partial^4 v_0}{\partial x^2\partial y\,\partial t}-A_y^2\frac{\partial^5 w}{\partial x^2\partial y^2\partial t}+\upsilon\left(A_x^1\frac{\partial^4 u_0}{\partial x^3\partial t}-A_x^2\frac{\partial^5 w}{\partial x^4\partial t}\right)\right) \\ -\tau_d\ell^2\left(\begin{array}{l} A_y^1\frac{\partial^6 v_0}{\partial x^4\partial y\,\partial t}-A_y^2\frac{\partial^7 w}{\partial x^4\partial y^2\partial t}+\upsilon\left(A_x^1\frac{\partial^6 u_0}{\partial x^5\partial t}-A_x^2\frac{\partial^7 w}{\partial x^6\partial t}\right) \\ +A_y^1\frac{\partial^6 v_0}{\partial x^2\partial y^3\partial t}-A_y^2\frac{\partial^7 w}{\partial x^2\partial y^4\partial t}+\upsilon\left(A_x^1\frac{\partial^6 u_0}{\partial x^3\partial y^2\partial t}-A_x^2\frac{\partial^7 w}{\partial x^4\partial y^2\partial t}\right) \end{array}\right) \end{array}\right)$$
$$+\frac{(e_0a)^2}{1-\upsilon^2}\times$$
$$\left(\begin{array}{l} A_y^1\frac{\partial^3 v_0}{\partial y^3}-A_y^2\frac{\partial^4 w}{\partial y^4}+\upsilon\left(A_x^1\frac{\partial^3 u_0}{\partial x\partial y^2}-A_x^2\frac{\partial^4 w}{\partial x^2\partial y^2}\right) \\ -\ell^2\left(\begin{array}{l} A_y^1\frac{\partial^5 v_0}{\partial x^2\partial y^3}-A_y^2\frac{\partial^6 w}{\partial x^2\partial y^4}+\upsilon\left(A_x^1\frac{\partial^5 u_0}{\partial x^3\partial y^2}-A_x^2\frac{\partial^6 w}{\partial x^4\partial y^2}\right) \\ +A_y^1\frac{\partial^5 v_0}{\partial y^5}-A_y^2\frac{\partial^6 w}{\partial y^6}+\upsilon\left(A_x^1\frac{\partial^5 u_0}{\partial x\partial y^4}-A_x^2\frac{\partial^6 w}{\partial x^2\partial y^4}\right) \end{array}\right) \\ +\tau_d\left(A_y^1\frac{\partial^4 v_0}{\partial y^3\partial t}-A_y^2\frac{\partial^5 w}{\partial y^4\partial t}+\upsilon\left(A_x^1\frac{\partial^4 u_0}{\partial x\partial y^2\partial t}-A_x^2\frac{\partial^5 w}{\partial x^2\partial y^2\partial t}\right)\right) \\ -\tau_d\ell^2\left(\begin{array}{l} A_y^1\frac{\partial^6 v_0}{\partial x^2\partial y^3\partial t}-A_y^2\frac{\partial^7 w}{\partial x^2\partial y^4\partial t}+\upsilon\left(A_x^1\frac{\partial^6 u_0}{\partial x^3\partial y^2\partial t}-A_x^2\frac{\partial^7 w}{\partial x^4\partial y^2\partial t}\right) \\ +A_y^1\frac{\partial^6 v_0}{\partial y^5\partial t}-A_y^2\frac{\partial^7 w}{\partial y^6\partial t}+\upsilon\left(A_x^1\frac{\partial^6 u_0}{\partial x\partial y^4\partial t}-A_x^2\frac{\partial^7 w}{\partial x^2\partial y^4\partial t}\right) \end{array}\right) \end{array}\right) \quad \text{(A.5)}$$
$$-e_{32}\left(-C^1\beta'\phi_E-B^1\frac{2V_E}{h}\right)+\frac{(e_0a)^2}{1-\upsilon^2}\left(-e_{32}\left(-C^1\beta'\frac{\partial^2\phi_E}{\partial x^2}\right)-e_{32}\left(-C^1\beta'\frac{\partial^2\phi_E}{\partial y^2}\right)\right)$$

$$M_{xy} =$$
$$\left(\begin{array}{l} A_{xy}^1\frac{\partial u_0}{\partial y}+A_{xy}^1\frac{\partial v_0}{\partial x}-2A_{xy}^2\frac{\partial^2 w}{\partial x\,\partial y} \\ -\ell^2\left(\begin{array}{l} A_{xy}^1\frac{\partial^3 u_0}{\partial x^2\partial y}+A_{xy}^1\frac{\partial^3 v_0}{\partial x^3}-2A_{xy}^2\frac{\partial^4 w}{\partial x^3\partial y} \\ +A_{xy}^1\frac{\partial^3 u_0}{\partial y^3}+A_{xy}^1\frac{\partial^3 v_0}{\partial x\partial y^2}-2A_{xy}^2\frac{\partial^4 w}{\partial x\partial y^3} \end{array}\right) \\ +\tau_d\left(A_{xy}^1\frac{\partial^2 u_0}{\partial y\,\partial t}+A_{xy}^1\frac{\partial^2 v_0}{\partial x\,\partial t}-2A_{xy}^2\frac{\partial^3 w}{\partial x\,\partial y\,\partial t}\right) \\ -\tau_d\ell^2\left(\begin{array}{l} A_{xy}^1\frac{\partial^4 u_0}{\partial x^2\partial y\,\partial t}+A_{xy}^1\frac{\partial^4 v_0}{\partial x^3\partial t}-2A_{xy}^2\frac{\partial^5 w}{\partial x^3\partial y\,\partial t} \\ +A_{xy}^1\frac{\partial^4 u_0}{\partial y^3\partial t}+A_{xy}^1\frac{\partial^4 v_0}{\partial x\partial y^2\partial t}-2A_{xy}^2\frac{\partial^5 w}{\partial x\partial y^3\partial t} \end{array}\right) \end{array}\right) \quad \text{(A.6)}$$
$$+(e_0a)^2$$
$$\left(\begin{array}{l} A_{xy}^1\frac{\partial^3 u_0}{\partial x^2\partial y}+A_{xy}^1\frac{\partial^3 v_0}{\partial x^3}-2A_{xy}^2\frac{\partial^4 w}{\partial x^3\partial y} \\ -\ell^2\left(\begin{array}{l} A_{xy}^1\frac{\partial^5 u_0}{\partial x^4\partial y}+A_{xy}^1\frac{\partial^5 v_0}{\partial x^5}-2A_{xy}^2\frac{\partial^6 w}{\partial x^5\partial y} \\ +A_{xy}^1\frac{\partial^5 u_0}{\partial x^2\partial y^3}+A_{xy}^1\frac{\partial^5 v_0}{\partial x^3\partial y^2}-2A_{xy}^2\frac{\partial^6 w}{\partial x^3\partial y^3} \end{array}\right) \\ +\tau_d\left(A_{xy}^1\frac{\partial^4 u_0}{\partial x^2\partial y\,\partial t}+A_{xy}^1\frac{\partial^4 v_0}{\partial x^3\partial t}-2A_{xy}^2\frac{\partial^5 w}{\partial x^3\partial y\,\partial t}\right) \\ -\tau_d\ell^2\left(\begin{array}{l} A_{xy}^1\frac{\partial^6 u_0}{\partial x^4\partial y\,\partial t}+A_{xy}^1\frac{\partial^6 v_0}{\partial x^5\partial t}-2A_{xy}^2\frac{\partial^7 w}{\partial x^5\partial y\,\partial t} \\ +A_{xy}^1\frac{\partial^6 u_0}{\partial x^2\partial y^3\partial t}+A_{xy}^1\frac{\partial^6 v_0}{\partial x^3\partial y^2\partial t}-2A_{xy}^2\frac{\partial^7 w}{\partial x^3\partial y^3\partial t} \end{array}\right) \end{array}\right) \quad \text{(A.6)}$$
$$+(e_0a)^2$$
$$\left(\begin{array}{l} A_{xy}^1\frac{\partial^3 u_0}{\partial y^3}+A_{xy}^1\frac{\partial^3 v_0}{\partial x\partial y^2}-2A_{xy}^2\frac{\partial^4 w}{\partial x\partial y^3} \\ -\ell^2\left(\begin{array}{l} A_{xy}^1\frac{\partial^5 u_0}{\partial x^2\partial y^3}+A_{xy}^1\frac{\partial^5 v_0}{\partial x^3\partial y^2}-2A_{xy}^2\frac{\partial^6 w}{\partial x^3\partial y^3} \\ +A_{xy}^1\frac{\partial^5 u_0}{\partial y^5}+A_{xy}^1\frac{\partial^5 v_0}{\partial x\partial y^4}-2A_{xy}^2\frac{\partial^6 w}{\partial x\partial y^5} \end{array}\right) \\ +\tau_d\left(A_{xy}^1\frac{\partial^4 u_0}{\partial y^3\partial t}+A_{xy}^1\frac{\partial^4 v_0}{\partial x\partial y^2\partial t}-2A_{xy}^2\frac{\partial^5 w}{\partial x\partial y^3\partial t}\right) \\ -\tau_d\ell^2\left(\begin{array}{l} A_{xy}^1\frac{\partial^6 u_0}{\partial x^2\partial y^3\partial t}+A_{xy}^1\frac{\partial^6 v_0}{\partial x^3\partial y^2\partial t}-2A_{xy}^2\frac{\partial^7 w}{\partial x^3\partial y^3\partial t} \\ +A_{xy}^1\frac{\partial^6 u_0}{\partial y^5\partial t}+A_{xy}^1\frac{\partial^6 v_0}{\partial x\partial y^4\partial t}-2A_{xy}^2\frac{\partial^7 w}{\partial x\partial y^5\partial t} \end{array}\right) \end{array}\right)$$
$$\overline{D}_x=\xi_{11}D^0\frac{\partial\phi_E}{\partial x}+(ea)^2\left(\xi_{11}D^0\frac{\partial^3\phi_E}{\partial x^3}+\xi_{11}D^0\frac{\partial^3\phi_E}{\partial x\partial y^2}\right)$$
$$\overline{D}_y=\xi_{22}D^0\frac{\partial\phi_E}{\partial y}+(ea)^2\left(\xi_{22}D^0\frac{\partial^3\phi_E}{\partial x^2\partial y}+\xi_{22}D^0\frac{\partial^3\phi_E}{\partial y^3}\right)$$
$$\overline{D}_z=e_{31}\left(B^0\frac{\partial u_0}{\partial x}-B^1\frac{\partial^2 w}{\partial x^2}\right)$$
$$+e_{32}\left(B^0\frac{\partial v_0}{\partial y}-B^1\frac{\partial^2 w}{\partial y^2}\right)+\xi_{33}\left(-\beta'C^0\phi_E-B^0\frac{2V_E}{h}\right) \quad \text{(A.7)}$$
$$+(e_0a)^2\left(e_{31}\left(B^0\frac{\partial^3 u_0}{\partial x^3}-B^1\frac{\partial^4 w}{\partial x^4}\right)+e_{32}\left(B^0\frac{\partial^3 v_0}{\partial x^2\partial y}-B^1\frac{\partial^4 w}{\partial x^2\partial y^2}\right)+\xi_{33}\left(-\beta'C^0\frac{\partial^2\phi_E}{\partial x^2}\right)\right)$$
$$+(e_0a)^2\left(e_{31}\left(B^0\frac{\partial^3 u_0}{\partial x\partial y^2}-B^1\frac{\partial^4 w}{\partial x^2\partial y^2}\right)+e_{32}\left(B^0\frac{\partial^3 v_0}{\partial y^3}-B^1\frac{\partial^4 w}{\partial y^4}\right)+\xi_{33}\left(-\beta'C^0\frac{\partial^2\phi_E}{\partial y^2}\right)\right)$$

Appendix B

$$
k_{11}=\begin{pmatrix} A_x^0\left(\frac{1}{1-\upsilon^2}\right)\left(-\alpha^2-\ell^2(\alpha^4+\alpha^2\beta^2)+(ea)^2\begin{pmatrix}\alpha^4-\ell^2(-\alpha^6-\alpha^4\beta^2)\\ +\alpha^2\beta^2-\ell^2(-\alpha^4\beta^2-\alpha^2\beta^4)\end{pmatrix}\right)\\ +A_{xy}^0\left(-\beta^2-\ell^2(\alpha^2\beta^2+\beta^4)+(ea)^2\begin{pmatrix}\alpha^2\beta^2-\ell^2(-\alpha^4\beta^2-\alpha^2\beta^4)\\ +\beta^4-\ell^2(-\alpha^2\beta^4-\beta^6)\end{pmatrix}\right)\end{pmatrix}
$$

$$
k_{12}=\begin{pmatrix} A_x^0(\frac{\upsilon}{1-\upsilon^2})\begin{pmatrix}-\alpha\beta-\ell^2(\alpha^3\beta+\alpha\beta^3)\\ +(ea)^2\begin{pmatrix}\alpha^3\beta-\ell^2(-\alpha^5\beta-\alpha^3\beta^3)\\ +\alpha\beta^3-\ell^2(-\alpha^3\beta^3-\alpha\beta^5)\end{pmatrix}\end{pmatrix}\\ +A_{xy}^0\begin{pmatrix}-\alpha\beta-\ell^2(\alpha^3\beta+\alpha\beta^3)\\ +(ea)^2\begin{pmatrix}\alpha^3\beta-\ell^2(-\alpha^5\beta-\alpha^3\beta^3)\\ +\alpha\beta^3-\ell^2(-\alpha^3\beta^3-\alpha\beta^5)\end{pmatrix}\end{pmatrix}\end{pmatrix}
$$

(B.1)

$$
k_{13}=\begin{pmatrix} A_x^1(\frac{1}{1-\upsilon^2})\begin{pmatrix}\alpha^3+\upsilon\alpha\beta^2-\ell^2(-\alpha^5-\upsilon\alpha^3\beta^2-\alpha^3\beta^2-\upsilon\alpha\beta^4)\\ +(ea)^2\begin{pmatrix}-\alpha^5-\upsilon\alpha^3\beta^2-\ell^2(\alpha^7+\upsilon\alpha^5\beta^2+\alpha^5\beta^2+\upsilon\alpha^3\beta^4)\\ -\alpha^3\beta^2-\upsilon\alpha\beta^4-\ell^2(\alpha^5\beta^2+\upsilon\alpha^3\beta^4+\alpha^3\beta^4+\upsilon\alpha\beta^6)\end{pmatrix}\end{pmatrix}\\ +2A_{xy}^1\left(\alpha\beta^2-\ell^2(-\alpha^3\beta^2-\alpha\beta^4)+(ea)^2\begin{pmatrix}-\alpha^3\beta^2-\ell^2(\alpha^5\beta^2+\alpha^3\beta^4)\\ -\alpha\beta^4-\ell^2(\alpha^3\beta^4+\alpha\beta^6)\end{pmatrix}\right)\end{pmatrix}
$$

$$
k_{14}=C^0e_{31}\beta'\alpha-((ea)^2)C^0e_{31}\beta 1(\alpha^3+\alpha\beta^2)
$$

$$
k_{21}=\begin{pmatrix} A_x^0(\frac{\upsilon}{1-\upsilon^2})\left(-\alpha\beta-\ell^2(\alpha^3\beta+\alpha\beta^3)+(ea)^2\begin{pmatrix}\alpha^3\beta-\ell^2(-\alpha^5\beta-\alpha^3\beta^3)\\ +\alpha\beta^3-\ell^2(-\alpha^3\beta^3-\alpha\beta^5)\end{pmatrix}\right)\\ +A_{xy}^0\left(-\alpha\beta-\ell^2(\alpha^3\beta+\alpha\beta^3)+(ea)^2\begin{pmatrix}\alpha^3\beta-\ell^2(-\alpha^5\beta-\alpha^3\beta^3)\\ +\alpha\beta^3-\ell^2(-\alpha^3\beta^3-\alpha\beta^5)\end{pmatrix}\right)\end{pmatrix}
$$

$$
k_{22}=\begin{pmatrix} A_y^0(\frac{1}{1-\upsilon^2}\left(-\beta^2-\ell^2(\beta^4+\alpha^2\beta^2)+(ea)^2\begin{pmatrix}\alpha^2\beta^2-\ell^2(-\alpha^2\beta^4-\alpha^4\beta^2)\\ +\beta^4-\ell^2(-\beta^6-\alpha^2\beta^4)\end{pmatrix}\right)\\ +A_{xy}^0\left(-\alpha^2-\ell^2(\alpha^2\beta^2+\alpha^4)+(ea)^2\begin{pmatrix}\alpha^4-\ell^2(-\alpha\beta^2-\alpha^6)\\ +\alpha^2\beta^2-\ell^2(-\alpha^2\beta^4-\alpha^4\beta^2)\end{pmatrix}\right)\end{pmatrix}
$$

(B.2)

$$
k_{23}=\begin{pmatrix} A_x^1(\frac{\upsilon}{1-\upsilon^2})\left(\alpha^2\beta-\ell^2(-\alpha^4\beta-\alpha^2\beta^3)+(ea)^2\begin{pmatrix}-\alpha^4\beta-\ell^2(\alpha^6\beta+\alpha^4\beta^3)\\ -\alpha^2\beta^3-\ell^2(\alpha^4\beta^3+\alpha^2\beta^5)\end{pmatrix}\right)\\ +A_y^1\frac{1}{1-\upsilon^2}\left(\beta^3-\ell^2(-\beta^5-\alpha^2\beta^3)+(ea)^2\begin{pmatrix}-\alpha^2\beta^3-\ell^2(\alpha^4\beta^3+\alpha^2\beta^5)\\ -\beta^5-\ell^2(\alpha^2\beta^5+\beta^7)\end{pmatrix}\right)\\ +2A_{xy}^1\left(\alpha^2\beta-(\ell^2)(-\alpha^4\beta-\alpha^2\beta^3)+(ea)^2\begin{pmatrix}-\alpha^4\beta-\ell^2(\alpha^6\beta+\alpha^4\beta^3)\\ -\alpha^2\beta^3-\ell^2(\alpha^4\beta^3+\alpha^2\beta^5)\end{pmatrix}\right)\end{pmatrix}
$$

$$
k_{24}=C^0e_{32}\beta'\beta-(ea)^2C^0e_{32}\beta_1(\beta^3+\alpha^2\beta)
$$

$$
k_{31}=\begin{pmatrix} A_x^1(\frac{1}{1-\upsilon^2})\begin{pmatrix}\alpha^3+\upsilon\alpha\beta^2-\ell^2(-\alpha^5-\upsilon\alpha^3\beta^2-\alpha^3\beta^2-\upsilon\alpha\beta^4)\\ +(ea)^2\begin{pmatrix}-\alpha^5-\upsilon\alpha^3\beta^2-\ell^2(\alpha^7+\upsilon\alpha^5\beta^2+\alpha^5\beta^2+\upsilon\alpha^3\beta^4)\\ -\alpha^3\beta^2-\upsilon\alpha\beta^4-\ell^2(\alpha^5\beta^2+\upsilon\alpha^3\beta^4+\alpha^3\beta^4+\upsilon\alpha\beta^6)\end{pmatrix}\end{pmatrix}\\ +2A_{xy}^1\left(\alpha\beta^2-\ell^2(-\alpha^3\beta^2-\alpha\beta^4)+(ea)^2\begin{pmatrix}-\alpha^3\beta^2-\ell^2(\alpha^5\beta^2+\alpha^3\beta^4)\\ -\alpha\beta^4-\ell^2(\alpha^3\beta^4+\alpha\beta^6)\end{pmatrix}\right)\end{pmatrix}
$$

$$
k_{32}=\begin{pmatrix} A_x^1(\frac{\upsilon}{1-\nu^2})\left(\alpha^2\beta-\ell^2(-\alpha^4\beta-\alpha^2\beta^3)+(ea)^2\begin{pmatrix}-\alpha^4\beta-\ell^2(\alpha^6\beta+\alpha^4\beta^3)\\ -\alpha^2\beta^3-\ell^2(\alpha^4\beta^3+\alpha^2\beta^5)\end{pmatrix}\right)\\ +A_y^1\frac{1}{1-\upsilon^2}\left(\beta^3-\ell^2(-\beta^5-\alpha^2\beta^3)+(ea)^2\begin{pmatrix}-\alpha^2\beta^3-\ell^2(\alpha^4\beta^3+\alpha^2\beta^5)\\ -\beta^5-\ell^2(\alpha^2\beta^5+\beta^7)\end{pmatrix}\right)\\ +2A_{xy}^1\left(\alpha^2\beta-(\ell^2)(-\alpha^4\beta-\alpha^2\beta^3)+(ea)^2\begin{pmatrix}-\alpha^4\beta-\ell^2(\alpha^6\beta+\alpha^4\beta^3)\\ -\alpha^2\beta^3-\ell^2(\alpha^4\beta^3+\alpha^2\beta^5)\end{pmatrix}\right)\end{pmatrix}
$$

(B.3)

$$k_{33}=\begin{pmatrix} A_x^2\frac{1}{1-\upsilon^2}\begin{pmatrix}-\alpha^4-\upsilon\alpha^2\beta^2-\ell^2(\alpha^6+\upsilon\alpha^4\beta^2+\alpha^4\beta^2+\upsilon\alpha^2\beta^4)\\ +(ea)^2\begin{pmatrix}\alpha^6+\upsilon\alpha^4\beta^2-\ell^2\begin{pmatrix}-\alpha^8-\upsilon\alpha^6\beta^2\\ -\alpha^6\beta^2-\upsilon\alpha^4\beta^4\end{pmatrix}\\ +\alpha^4\beta^2+\upsilon\alpha^2\beta^4-\ell^2\begin{pmatrix}-\alpha^6\beta^2-\upsilon\alpha^4\beta^4\\ -\alpha^4\beta^4-\upsilon\alpha^2\beta^6\end{pmatrix}\end{pmatrix}\end{pmatrix}\\ +\frac{1}{1-\upsilon^2}\begin{pmatrix}-A_y^2\beta^4-A_x^2\upsilon\alpha^2\beta^2-\ell^2\begin{pmatrix}A_y^2\alpha^2\beta^4+A_x^2\upsilon\alpha^4\beta^2\\ +A_y^2\beta^6+A_x^2\upsilon\alpha^2\beta^4\end{pmatrix}\\ +(ea)^2\begin{pmatrix}A_y^2\alpha^2\beta^4+A_x^2\upsilon\alpha^4\beta^2-\ell^2\begin{pmatrix}-A_y^2\alpha^4\beta^4-A_x^2\upsilon\alpha^6\beta^2\\ -A_y^2\alpha^2\beta^6-A_x^2\upsilon\alpha^4\beta^4\end{pmatrix}\\ +A_y^2\beta^6+A_x^2\upsilon\alpha^2\beta^4-\ell^2\begin{pmatrix}-A_y^2\alpha^2\beta^6-A_x^2\upsilon\alpha^4\beta^4\\ -A_y^2\beta^8-A_x^2\upsilon\alpha^2\beta^6\end{pmatrix}\end{pmatrix}\end{pmatrix}\\ +4A_{xy}^2\begin{pmatrix}-\alpha^2\beta^2-\ell^2(\alpha^4\beta^2+\alpha^2\beta^4)\\ +(ea)^2\begin{pmatrix}\alpha^4\beta^2-\ell^2(-\alpha^4\beta^4-\alpha^6\beta^2)\\ +\alpha^2\beta^4-\ell^2(-\alpha^4\beta^4-\alpha^2\beta^6)\end{pmatrix}\end{pmatrix}\end{pmatrix} \tag{B.3}$$

$$k_{34}=C^1e_{31}\beta'(-\alpha^2+(ea)^2(\alpha^4+\alpha^2\beta^2))+C^1e_{32}\beta'(-\beta^2+(ea)^2(\beta^4+\alpha^2\beta^2))$$

$$\begin{aligned}k_{41}&=0\\ k_{42}&=0\\ k_{43}&=0\\ k_{44}&=d_{11}D^0(-\alpha^2+(ea)^2(\alpha^4+\alpha^2\beta^2))+d_{22}D^0(-\beta^2+(ea)^2(\beta^4+\alpha^2\beta^2))\end{aligned} \tag{B.4}$$

$$c_{11}=\tau_d\begin{pmatrix}A_x^0\left(\frac{1}{1-\upsilon^2}\right)\left(-\alpha^2-\ell^2(\alpha^4+\alpha^2\beta^2)+(ea)^2\begin{pmatrix}\alpha^4-\ell^2(-\alpha^6-\alpha^4\beta^2)\\ +\alpha^2\beta^2-\ell^2(-\alpha^4\beta^2-\alpha^2\beta^4)\end{pmatrix}\right)\\ +A_{xy}^0\left(-\beta^2-\ell^2(\alpha^2\beta^2+\beta^4)+(ea)^2\begin{pmatrix}\alpha^2\beta^2-\ell^2(-\alpha^4\beta^2-\alpha^2\beta^4)\\ +\beta^4-\ell^2(-\alpha^2\beta^4-\beta^6)\end{pmatrix}\right)\end{pmatrix}$$

$$c_{12}=\tau_d\begin{pmatrix}A_x^0(\frac{\upsilon}{1-\upsilon^2})\begin{pmatrix}-\alpha\beta-\ell^2(\alpha^3\beta+\alpha\beta^3)\\ +(ea)^2\begin{pmatrix}\alpha^3\beta-\ell^2(-\alpha^5\beta-\alpha^3\beta^3)\\ +\alpha\beta^3-\ell^2(-\alpha^3\beta^3-\alpha\beta^5)\end{pmatrix}\end{pmatrix}\\ +A_{xy}^0\begin{pmatrix}-\alpha\beta-\ell^2(\alpha^3\beta+\alpha\beta^3)\\ +(ea)^2\begin{pmatrix}\alpha^3\beta-\ell^2(-\alpha^5\beta-\alpha^3\beta^3)\\ +\alpha\beta^3-\ell^2(-\alpha^3\beta^3-\alpha\beta^5)\end{pmatrix}\end{pmatrix}\end{pmatrix} \tag{B.5}$$

$$c_{13}=\tau_d\begin{pmatrix}A_x^1(\frac{1}{1-\upsilon^2})\begin{pmatrix}\alpha^3+\upsilon\alpha\beta^2-\ell^2(-\alpha^5-\upsilon\alpha^3\beta^2-\alpha^3\beta^2-\upsilon\alpha\beta^4)\\ +(ea)^2\begin{pmatrix}-\alpha^5-\upsilon\alpha^3\beta^2-\ell^2(\alpha^7+\upsilon\alpha^5\beta^2+\alpha^5\beta^2+\upsilon\alpha^3\beta^4)\\ -\alpha^3\beta^2-\upsilon\alpha\beta^4-\ell^2(\alpha^5\beta^2+\upsilon\alpha^3\beta^4+\alpha^3\beta^4+\upsilon\alpha\beta^6)\end{pmatrix}\end{pmatrix}\\ +2A_{xy}^1\left(\alpha\beta^2-\ell^2(-\alpha^3\beta^2-\alpha\beta^4)+(ea)^2\begin{pmatrix}-\alpha^3\beta^2-\ell^2(\alpha^5\beta^2+\alpha^3\beta^4)\\ -\alpha\beta^4-\ell^2(\alpha^3\beta^4+\alpha\beta^6)\end{pmatrix}\right)\end{pmatrix} \tag{B.5}$$

$$c_{14}=0$$

$$c_{21}=\tau_d\begin{pmatrix}A_x^0(\frac{\upsilon}{1-\upsilon^2})\left(-\alpha\beta-\ell^2(\alpha^3\beta+\alpha\beta^3)+(ea)^2\begin{pmatrix}\alpha^3\beta-\ell^2(-\alpha^5\beta-\alpha^3\beta^3)\\ +\alpha\beta^3-\ell^2(-\alpha^3\beta^3-\alpha\beta^5)\end{pmatrix}\right)\\ +A_{xy}^0\left(-\alpha\beta-\ell^2(\alpha^3\beta+\alpha\beta^3)+(ea)^2\begin{pmatrix}\alpha^3\beta-\ell^2(-\alpha^5\beta-\alpha^3\beta^3)\\ +\alpha\beta^3-\ell^2(-\alpha^3\beta^3-\alpha\beta^5)\end{pmatrix}\right)\end{pmatrix} \tag{B.6}$$

$$c_{22}=\tau_d\begin{pmatrix} A_y^0\left(\frac{1}{1-\upsilon^2}\right)\left(-\beta^2-\ell^2(\beta^4+\alpha^2\beta^2)+(ea)^2\begin{pmatrix}\alpha^2\beta^2-\ell^2(-\alpha^2\beta^4-\alpha^4\beta^2)\\+\beta^4-\ell^2(-\beta^6-\alpha^2\beta^4)\end{pmatrix}\right)\\ +A_{xy}^0\left(-\alpha^2-\ell^2(\alpha^2\beta^2+\alpha^4)+(ea)^2\begin{pmatrix}\alpha^4-\ell^2(-\alpha\beta^2-\alpha^6)\\+\alpha^2\beta^2-\ell^2(-\alpha^2\beta^4-\alpha^4\beta^2)\end{pmatrix}\right)\end{pmatrix}$$

$$c_{23}=\tau_d\begin{pmatrix} A_x^1\left(\frac{\upsilon}{1-\upsilon^2}\right)\left(\alpha^2\beta-\ell^2(-\alpha^4\beta-\alpha^2\beta^3)+(ea)^2\begin{pmatrix}-\alpha^4\beta-\ell^2(\alpha^6\beta+\alpha^4\beta^3)\\-\alpha^2\beta^3-\ell^2(\alpha^4\beta^3+\alpha^2\beta^5)\end{pmatrix}\right)\\ +A_y^1\frac{1}{1-\upsilon^2}\left(\beta^3-\ell^2(-\beta^5-\alpha^2\beta^3)+(ea)^2\begin{pmatrix}-\alpha^2\beta^3-\ell^2(\alpha^4\beta^3+\alpha^2\beta^5)\\-\beta^5-\ell^2(\alpha^2\beta^5+\beta^7)\end{pmatrix}\right)\\ +2A_{xy}^1\left(\alpha^2\beta-(\ell^2)(-\alpha^4\beta-\alpha^2\beta^3)+(ea)^2\begin{pmatrix}-\alpha^4\beta-\ell^2(\alpha^6\beta+\alpha^4\beta^3)\\-\alpha^2\beta^3-\ell^2(\alpha^4\beta^3+\alpha^2\beta^5)\end{pmatrix}\right)\end{pmatrix} \tag{B.6}$$

$$c_{24}=0$$

$$c_{31}=\tau_d\begin{pmatrix} A_x^1\left(\frac{1}{1-\upsilon^2}\right)\left(\alpha^3+\upsilon\alpha\beta^2-\ell^2(-\alpha^5-\upsilon\alpha^3\beta^2-\alpha^3\beta^2-\upsilon\alpha\beta^4)\right.\\ \left.+(ea)^2\begin{pmatrix}-\alpha^5-\upsilon\alpha^3\beta^2-\ell^2(\alpha^7+\upsilon\alpha^5\beta^2+\alpha^5\beta^2+\upsilon\alpha^3\beta^4)\\-\alpha^3\beta^2-\upsilon\alpha\beta^4-\ell^2(\alpha^5\beta^2+\upsilon\alpha^3\beta^4+\alpha^3\beta^4+\upsilon\alpha\beta^6)\end{pmatrix}\right)\\ +2A_{xy}^1\left(\alpha\beta^2-\ell^2(-\alpha^3\beta^2-\alpha\beta^4)+(ea)^2\begin{pmatrix}-\alpha^3\beta^2-\ell^2(\alpha^5\beta^2+\alpha^3\beta^4)\\-\alpha\beta^4-\ell^2(\alpha^3\beta^4+\alpha\beta^6)\end{pmatrix}\right)\end{pmatrix}$$

$$c_{32}=\tau_d\begin{pmatrix} A_x^1\left(\frac{\upsilon}{1-\upsilon^2}\right)\left(\alpha^2\beta-\ell^2(-\alpha^4\beta-\alpha^2\beta^3)+(ea)^2\begin{pmatrix}-\alpha^4\beta-\ell^2(\alpha^6\beta+\alpha^4\beta^3)\\-\alpha^2\beta^3-\ell^2(\alpha^4\beta^3+\alpha^2\beta^5)\end{pmatrix}\right)\\ +A_y^1\frac{1}{1-\upsilon^2}\left(\beta^3-\ell^2(-\beta^5-\alpha^2\beta^3)+(ea)^2\begin{pmatrix}-\alpha^2\beta^3-\ell^2(\alpha^4\beta^3+\alpha^2\beta^5)\\-\beta^5-\ell^2(\alpha^2\beta^5+\beta^7)\end{pmatrix}\right)\\ +2A_{xy}^1\left(\alpha^2\beta-(\ell^2)(-\alpha^4\beta-\alpha^2\beta^3)+(ea)^2\begin{pmatrix}-\alpha^4\beta-\ell^2(\alpha^6\beta+\alpha^4\beta^3)\\-\alpha^2\beta^3-\ell^2(\alpha^4\beta^3+\alpha^2\beta^5)\end{pmatrix}\right)\end{pmatrix} \tag{B.7}$$

$$c_{33}=\tau_d\begin{pmatrix} A_x^2\frac{1}{1-\upsilon^2}\begin{pmatrix}-\alpha^4-\upsilon\alpha^2\beta^2-\ell^2(\alpha^6+\upsilon\alpha^4\beta^2+\alpha^4\beta^2+\upsilon\alpha^2\beta^4)\\+(ea)^2\begin{pmatrix}\alpha^6+\upsilon\alpha^4\beta^2-\ell^2\begin{pmatrix}-\alpha^8-\upsilon\alpha^6\beta^2\\-\alpha^6\beta^2-\upsilon\alpha^4\beta^4\end{pmatrix}\\+\alpha^4\beta^2+\upsilon\alpha^2\beta^4-\ell^2\begin{pmatrix}-\alpha^6\beta^2-\upsilon\alpha^4\beta^4\\-\alpha^4\beta^4-\upsilon\alpha^2\beta^6\end{pmatrix}\end{pmatrix}\end{pmatrix}\\ +\frac{1}{1-\upsilon^2}\begin{pmatrix}-A_y^2\beta^4-A_x^2\upsilon\alpha^2\beta^2-\ell^2\begin{pmatrix}A_y^2\alpha^2\beta^4+A_x^2\upsilon\alpha^4\beta^2\\+A_y^2\beta^6+A_x^2\upsilon\alpha^2\beta^4\end{pmatrix}\\+(ea)^2\begin{pmatrix}A_y^2\alpha^2\beta^4+A_x^2\upsilon\alpha^4\beta^2-\ell^2\begin{pmatrix}-A_y^2\alpha^4\beta^4-A_x^2\upsilon\alpha^6\beta^2\\-A_y^2\alpha^2\beta^6-A_x^2\upsilon\alpha^4\beta^4\end{pmatrix}\\+A_y^2\beta^6+A_x^2\upsilon\alpha^2\beta^4-\ell^2\begin{pmatrix}-A_y^2\alpha^2\beta^6-A_x^2\upsilon\alpha^4\beta^4\\-A_y^2\beta^8-A_x^2\upsilon\alpha^2\beta^6\end{pmatrix}\end{pmatrix}\end{pmatrix}\\ +4A_{xy}^2\begin{pmatrix}-\alpha^2\beta^2-\ell^2(\alpha^4\beta^2+\alpha^2\beta^4)\\+(ea)^2\begin{pmatrix}\alpha^4\beta^2-\ell^2(-\alpha^4\beta^4-\alpha^6\beta^2)\\+\alpha^2\beta^4-\ell^2(-\alpha^4\beta^4-\alpha^2\beta^6)\end{pmatrix}\end{pmatrix}\end{pmatrix} \tag{B.7}$$

$$c_{34}=0$$

$$\begin{aligned} c_{41} &= 0 \\ c_{42} &= 0 \\ c_{43} &= 0 \\ c_{44} &= 0 \end{aligned} \tag{B.8}$$

$$\begin{cases} m_{11} = I^0 & m_{21} = 0 & m_{31} = -I^1\alpha & m_{41} = 0 \\ m_{12} = 0 & m_{22} = I^0 & m_{32} = -I^1\beta & m_{42} = 0 \\ m_{13} = -I^1\alpha & m_{23} = -I^1\beta & m_{33} = I^2(\alpha^2+\beta^2) + I^1 & m_{43} = 0 \\ m_{14} = 0 & m_{24} = 0 & m_{34} = 0 & m_{44} = 0 \end{cases} \tag{B.9}$$